1993

Ultrastructure and Mitosis of Glaucosphaera vacuolata

Steven Philip Allan Goss
College of William & Mary - Arts & Sciences

Ultrastructure and Mitosis of *Glaucosphaera vacuolata*

A Thesis

Presented to

The Faculty of the Department of Biology

The College of William and Mary in Virginia

In Partial Fulfillment

Of the Requirements for the Degree of

Master of Arts

---

by

Steven Philip Allan Goss

1993

APPROVAL SHEET

This thesis is submitted in partial fulfillment of

the requirements for the degree of

Master of Arts

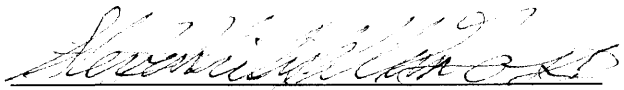

Author

Approved, July 1993

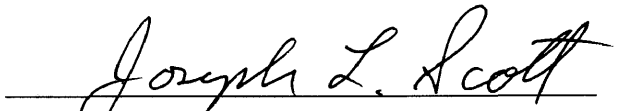

Joseph L. Scott

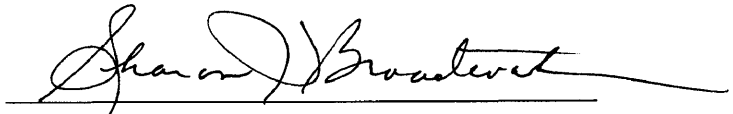

Sharon T. Broadwater

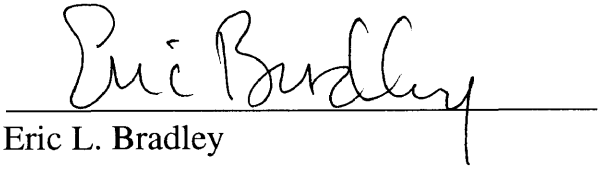

Eric L. Bradley

DEDICATION

To my parents and brother, who have shown me the strength and courage to prevail upon that which is set before me, and the knowledge that they will never be further than a phone call away.

TABLE OF CONTENTS

ACKNOWLEDGMENTS

I would like to express my sincere gratitude to both Dr. Joseph L. Scott and Dr. Sharon T. Broadwater for their patience, expertise and friendship. I thank Dr. Eric Bradley for serving on my comittee and critically reviewing the manuscript during a very chaotic time. I would like to express my fullest appreciation to both Bill Saunders and Jewel Thomas for their technical assistance, guidance and encouragement. I can not fully express my indebtedness and gratitude for the help and support provided by these people, my friends and especially my family.

LIST OF TABLES

LIST OF FIGURES

ABSTRACT

This investigation of the vegetative and mitotic ultrastructure of *Glaucosphaera vacuolata* proposes a change in this organism's taxonomic position. Although considered a member of the Glaucophyta by many, *Glaucosphaera vacuolata* lacks most of the common characteristics exhibited by this phylum. The Glaucophyta is composed of colorless host cells which contain individual cyanelles (endosymbiotic cyanobacteria with reduced cell walls). These organisms also have flagella, a pellicular-lacunae system and parabasal Golgi bodies. In contrast, *Glaucosphaera* cells have a single, multi-lobed chloroplast, a peripheral ER-tubule system, perinuclear Golgi bodies which undergo intercisternal fusion and have no flagellar apparatus. These traits of *Glaucosphaera* are all indicative of Rhodophytan affinity. In addition, a thorough investigation of the mitotic process shows that unlike the Glaucophyta, *Glaucosphaera* has a closed mitotic spindle and displays aspects of mitosis similar to those of red algae. At prophase, a large microtubule organizing center (MTOC) is present at each pole but does not appear to have a nucleus-associated organelle (NAO). All subsequent stages are similar to those reported for red algal unicells. The only major differences in mitosis between *Glaucosphaera* and the red algal unicells are the absence of typical ring-shaped NAOs, a mixing of chromatin and nucleolar material during anaphase and well defined kinetochores in *Glaucosphaera*. Even with these differences, our results suggest that *Glaucosphaera* is better placed in the Rhodophyta than the Glaucophyta.

Ultrastructure and Mitosis of *Glaucosphaera vacuolata*

INTRODUCTION

The protistan phylum, Rhodophyta, has historically caused considerable debate among phycologists. Since the original classification into taxonomic groups according to color variation by Lamouroux in 1813, there have been many changes in rhodophytan taxonomy. This diverse group of organisms share few ultrastructural and biochemical features among all of its members. Those few shared include: lack of a centriole complex at all times in its life history; chloroplasts with unstacked thylakoids to which are attached accessory phycobilin pigment-containing structures known as phycobilisomes; a persistent nuclear envelope during mitosis; and starch storage deposits free in the cytoplasm of the cell (Gabrielson and Garbary 1986, Garbary and Gabrielson 1990). The main problem classifying organisms within this phylum is a result of the difficulty in choosing characteristics with which to delineate the members at each taxonomic level.

Until recently, classification within the Rhodophyta was based upon gross and light microscopic morphological characteristics and life history of each organism. With the advent of biochemistry, molecular biology and electron microscopy, many of these previously created groups have become questioned. The choice of characteristics upon which to base a valid taxonomic system has now expanded. Mitosis and pit plug development and ultrastructure have recently been proposed as important phylogenetic indicators, primarily due to their largely conservative nature (Scott *et al* 1980; Gabrielson and Garbary 1986).

It has been widely accepted that the red algae are a monophyletic group, meaning that they are all derived from a single ancestor. Presently there is but one class, the Rhodophyceae, recognized within the phylum. The Rhodophyta traditionally included two subclasses, the Florideophycidae and the Bangiophycidae (Garbary *et al.* 1980; Garbary and Gabrielson 1990; Gabrielson and Garbary 1986). The monophyletic subclass, Florideophycidae, was characterized by the presence of tetrasporangia and filamentous carposporophytes. The Bangiophycidae was a polyphyletic and paraphyletic subclass. This meant it was possible that its members not only originated from multiple ancestors, but each group derived from a common ancestor may not have included all the descendants (Garbary *et al.* 1980; Gabrielson and Garbary 1987). Since there were no shared derived characteristics with which its members may be united, this second subclass presented many taxonomic problems and was viewed as artificial (Lee 1980; Garbary and Gabrielson 1990).

According to Garbary and Gabrielson (1990), there are fifteen orders within the Rhodophyceae. The use of electron microscopy has demonstrated that cellular features, such as organelle associations and mitosis, indicate the possible artificial status of some of these orders. Detailed investigation into the mitotic and ultrastructural variations within each of these groups is necessary in order to determine the validity of these features as phylogenetic indicators.

Porphyridiales is an order of red algae that continues to be one of the most controversial within the Rhodophyta. This order is composed of unicellular organisms either free living or grouped into loosely arranged aggregations of cells within a mucilaginous matrix. In 1984, Scott presented evidence that variations in certian ultrastructural features of red algae are valid indicators of phylogenetic status, in particular, those pertaining to Golgi bodies, chloroplasts and cell division. Scott (1986) demonstrated further evidence of the apparent polyphyletic

nature of the Porphyridales when one of its freshwater members, *Flintiella sanguinaria*, was found to have mitotic characteristics differing from other unicells but closely related to that of another freshwater alga, *Batrachospermum* (Scott 1983). This latter organism belongs to the monophyletic order Batrachospermales, an order composed of multicellular algae of similar life history, ecological distribution and pit plug cap morphology. *Flintiella* mitosis did not as closely match that of *Porphyridium*, also of the Porphyridiales, suggesting that *Flintiella* may have evolved from a *Batrachospermum*-like organism.

Currently, only five members of the Porphyridiales have undergone thorough mitotic studies: *Porphyridium purpureum* (Schornstein and Scott 1982), *Flintiella sanguinaria* (Scott 1986), *Rhodella maculata* and *R. violacea* (Patrone *et al.* 1991) and *Dixoniella grisea* (Scott *et al.* 1992). Due to its polyphyletic nature, the members of this group do not demonstrate any unusual mitotic characteristics unto themselves, but they do show many similar characteristics that are highly variable within the Rhodophyta. All five unicells have polar gaps in the nuclear membrane, kinetochores (albeit, usually fairly indistinct), and lack perinuclear endoplasmic recticulum (PER). The only major differences include both interzonal spindle length and the appearance and behavior of nucleus associated organelles (NAOs) (Broadwater and Scott, in press). With the exception of *P. purpureum*, all investigated members have a NAO in the form of hollow cylinders of varying diameter called "polar rings". The NAO of *P. purpureum* is unusual in being a bipartite structure that consists of a small distal and large proximal portion (Schornstein and Scott 1982).

The Porphyridiales consists of two families, differentiated by chloroplast structure and presence or absence of a pyrenoid (Garbary and Gabrielson 1986). Members of the Porphyridiaceae contain a central pyrenoid and a single stellate chloroplast. Pyrenoids are absent in the Phragmonemataceae, a family that

contains either a single, highly lobed chloroplast or one to many discoid to lobed plastids (Garbary *et al.* 1980).

The enigmatic unicellular alga, *Glaucosphaera vacuolata*, has been proposed to be a member of the Porphyridiales (McCracken *et al.* 1980; Broadwater and Scott in press). This unicell was originally isolated in 1929 from the plankton of a meadow pond located near Kharkov (USSR). Using available light microscopic techniques on a limited sample (two stained cells), *Glaucosphaera* was classified and placed within the Glaucophyta by Korschikov (1930). The Glaucophyta is composed of apochlorotic organisms that obtain their nutrition through organelle-like endosymbionts termed cyanelles by Pascher (1929). With the exception of *Glauosphaera*, all cyanelles contained within the various genera of this phylum are surrounded by a reduced cell wall enclosed within a vesicle of the host cell (Kies and Kremer 1990) and do not lyse when isolated from the cell (Trench 1982). Of the glaucophytan genera studied thus far, *Glauosphaera* is unique by being devoid of a centriole complex at all times during its life cycle, lacking both persistent contractile vacuoles and an apical depression, having perinuclear dictyosomes that undergo intercisternal fusion, the presence of the red algal pigment R-phycocyanin and a persistent nuclear membrane during mitosis (Richardson and Brown 1970; Kies 1984; Garbary and Gabrielson 1990; Broadwater and Scott in press).

The purpose of this study is to present a through ultrastructural survey of both vegetative and mitotic cells illustrating the possible taxonomically important characteristics of *Glaucosphaera vacuolata*. Only two previous, somewhat comprehensive, ultrastructural investigations have been centered on this strange unicell and have have lead to contradicting results as to both the biochemical and ultrastructural characteristics (Richardson and Brown 1970; McCracken *et al.* 1980). Overall, the cellular features of *Glaucosphaera* closely match that of the

members of the Porphyridiales, specifically the family Phragmonemataceae. This, along with the lack of common characteristics shared within the Glaucophyta, suggests that *Glaucosphaera vacuolata* has been incorrectly classified and should to be included within the Phragmonemataceae of the Rhodophyta.

MATERIALS AND METHODS

Glaucosphaera vacuolata was obtained from the Culture Collection of Algae at the University of Texas at Austin (UTEX LB 1662). Stock cultures were maintained in 1000 mL modified *Volvox*-medium (Richardson and Brown 1970) in a covered 4000 mL Erlenmeyer Pyrex flask, incubated at 19-21°C with a 14-10 L/D photo period of approximately 1100 lux illumination. All stock and experimental cultures were oscillated on a shaker table at 100 rpm.

To approximate the time of log phase initiation, a culture was inoculated with cells, achieving a concentration of $1x10^6$ cells·L^{-1}, and placed in a photoperiod regime of 14-10 L/D. Using a hemocytometer, the numbers of cells were counted at the hour of inoculation over the following 19 days. To determine the peak hour of division, cells from the previous study were subcultured into 1000 mL *Volvox*-medium. This second culture contained approximately $17x10^6$ cells·L^{-1} as determined by hemocytometer count. After growing in the above conditions for four days, when the cells in the new culture approximated $35x10^6$ cells·L^{-1}, a 5 mL sample was procured from the culture every 20 min over 24 hrs. Each sample was immediately centrifuged at a setting of 5 for 60 sec, on a International Clinical Centrifuge, model CL. The supernatant was reduced to 1 mL and the pellet was re-suspended with 1 mL of Perfix (Fisher) using a Vortex Jr. Mixer (Scientific Industries Inc.). Cells were refrigerated at approximately 6 °C for 24 hr, rinsed and stored in McIlvane's buffer with a pH of 6.1. The number of cells undergoing cytokinesis in each sample was determined through cell counts. Cells were

photographed using Normarski differential interference and bright field optics on an Olympus BH-2 Photomicroscope.

Living and fixed cells were also observed with an Olympus BH2-RFK epi-UV illumination microscope equiped with a high pressure mercury vapor lamp. The DNA fluorochrome 4',6-diamidino-2-phenylindole (DAPI) was used in combination with exciter filter UG-1, dichroic mirror DM-400 (Goff and Coleman 1990) and 1,4-diazabicyclo-[2.2.2]-octane (DABCO) to view both cyanelle and nuclear DNA with minimal fading (Picciolo and Kaplan 1984). Both sunlight and Carnoy's solution (Goff and Coleman 1984) were used to reduce auto-fluorescence.

Cells were subcultured for electron microscopy and grown as before. On day 4 of growth, 4 fixations were made at 20 min intervals beginning on the eighth hour of the light period . For each sample, 6 mL of cells in culture media were suspended in 2 mL of 8% glutaraldehyde (making a 2% glutaraldehyde solution) at room temperature for 2 hr. After 3 rinses in culture media, cells were filtered onto polylysine coated Millipore filters, post-fixed with 1% OsO_4 in culture media for 1.5 hr at 6 °C and rinsed twice in culture media. Dehydration took place in a graded series of acetone solutions. Each sample was stained with 2% uranyl acetate in methanol for 20 hr during dehydration and embedded in EMBED 812. Thin sections of approximately 70 nm and thick sections of approximately 0.50 μm were serially sectioned with a diamond knife using an LKB Ultotome III and MT6000-XL RMC Ultramicrotome. Thin sections were post-stained with lead acetate and collected on fomvar coated one-hole grids to be examined with a Zeiss EM-109 electron microscope. Thick sections were collected on fomvar coated 100 and 300 mesh grids and examined on a Zeiss CEM-902 electron microscope equipped with a EELS spectrophotometer.

RESULTS

The population of *Glaucosphaera vacuolata,* inoculated to determine the time of log phase initiation, followed a typical growth curve (Fig. 1); however, the carrying capacity had not been reached by the end of the study. The total number of cells within the population was calculated daily at the inoculation hour, until well into the log phase of its life cycle. A separate culture was inoculated with these cells in order to determine the peak hour of division during log phase. The culture was monitored until the population roughly doubled in size. Samples were then procured at 20 min intervals, beginning at the hour of inoculation. The percentage of cells undergoinging cytokinesis, out of approximately 500, was calculated for each sample. Table 1 shows the data obtained from the study. A graph of the table (Fig. 2) illustrates that cells began to divide approximately five hours after the light period began and continued until roughly six hours into the dark period. The photoperiod regime was set at 14-10 L/D. The peak of mitotic activity occurred during the end of the seventh hour of the light period. This peak, however, only consisted of 2.6% of the cells undergoing cytokinesis.

Light Microscopy:

Glaucosphaera vacuolata is a spherical cell, averaging 17-26 μm in diameter. When cells are concentrated, they appear widely but evenly spaced (Fig. 3). The cause of this distribution pattern is a large mucilaginous sheath, which can be observed with the use of India Ink (Figs. 4-5). Sheath thickness of unicellular red algae varies both with cell age and culture conditions (Schornstein and Scott

1982; Broadwater and Scott in press). In *Glaucosphaera* the sheath averages 9 μm from the periphery of the cell to its border. This sheath does not appear in fixations for the electron microscope (Fig. 14).

With the use of fluorescence microscopy, the cells demonstrate considerable autofluorescence (Fig. 6). Fluorescent light is absorbed by the photosynthetic pigments within the chloroplast, exciting their electrons and causing them to jump into higher energy levels. When these fall back into their original locations, they release their kinetic energy in the form of a longer wavelength of light, thereby causing the chloroplasts to fluoresce. The DNA fluorochrome DAPI was used to localize DNA. Figures 7-13 demonstrates that the location of chloroplast DNA is usually in the periphery of the plastid, closest to the outer region of the cell. If the centers of cells stained with DAPI are brought into focus, nuclear DNA may be viewed. During both interphase and prophase, the DNA appears as a large diffuse area within the center of the cell (Fig. 8). Metaphase is marked by the congression of DNA into a localized, flattened plate (Fig. 9). Figures 10 and 11 illustrate the movement of chromatin towards the poles of the nucleus during anaphase. Telophase (Fig. 12) is shown when the DNA disperses into two, larger, diffuse areas, analogous to that of interphase. Cytokinesis appears to begin after the completion of telophase. A cleavage furrow appears in the cell, perpendicular to the plane of the division poles, and constricts until the daughter cells finally separate (Figs. 12-13).

Electron Microscopy:

Interphase:

Glaucosphaera does not possess a cell wall. Other than a mucilaginous sheath, it is limited only by a plasma membrane (Figs. 14, 15, 18). Located directly beneath the plasma membrane, throughout the circumference of the cell, is

a peripheral endoplasmic recticulum (PER) system. At irregular intervals, small tubules are frequently seen to arise from the peripheral ER and possibly fuse with the plasma membrane. The space between the plasma membrane and the peripheral ER is usually void of electron opaque material. Unfortunately, not all fixations of *Glaucosphaera* demonstrate this particular feature.

In select cells, osmiophilic spheres with a diameter of 120 nm, appearing similar to the viral particles found in *Porphyridium purpureum* by Chapman and Lang (1973), may be seen within the cytosol (Figs. 15-16). Other osmiophilic spheres, averaging 130-190 nm in diameter, are seen lying within the chloroplast (Figs. 17, 18, 23). These "eyespots", also referred to as plastoglobuli or stigmata, are hexagonally arranged into a single plate-like layer (Fig. 18). This layer is usually located in the periphery of the chloroplast, laying flat against the envelope in areas close to the outer region of the cell. When viewing live cells, these appear as reddish spots in the periphery of the chloroplast. The function of the stigmata is not clear, both because their location is not solely limited to one side of the cell and the cell has no apparent means of locomotion. Stigma-like bodies have, however, been found to exist in many red algal plastids (Deason *et al.* 1983; Pueschel 1990).

At high magnifications, a double membraned envelope can be seen limiting the chloroplast. Within the envelope, a peripheral, continuous thylakoid is always present. All thylakoids occur as single, unstacked membranes upon which are located the disk-shaped phycobilin pigment-containing structures termed phycobilisomes (Figs. 19-20). The general appearance of these structures, in a thin section, is similar to that of closely-placed coins standing on their edge upon the thylakoid membrane. Glancing sections of groups of phycobilisomes therefore tend to look like small cylinders rather than spheres, as seen in the center of Figure 19. Face views of phycobilisomes show that they can interdigitate with those

contained upon the facing thylakoid membrane, giving the thylakoids a zippered appearance (Fig. 20).

When cells are stored in Perfix (Fig. 21), interconnections can be seen between chloroplasts which are not usually distinct within live cells (Fig. 6). Electron microscopy better demonstrates these connections by showing what appear to be multiple chloroplasts that not only have connections, but at times share thylakoid membranes between each segment (Figs. 22-24).

Starch granules are not present in the chloroplast, but are scattered throughout the cytoplasm (Fig. 25). These may be distinguished from the many vacuoles present due to the lack of a limiting membrane (Figs. 27,28,40). Figure 28 shows the various morphological forms shown by the mitochondria within the cell. The regions of some mitochondria are compressed (Figs. 25-28), showing what has been thought to be a possible non-emergent, flagellar axonemal component (Scott, unpublished communication). Figure 26 shows a widening of these linear membranes, within which the cristae of mitochondria may be seen. These cristae, and those of the more typically shaped mitochondria, have a flattened appearance similar to those found in all red algal cells (Pueschel 1990; Broadwater and Scott in press). Figures 27 and 28 are serial sections showing how the layered region widens out into a typical mitochondrion.

A few cells contained a very unusual body. Figure 29 shows the relative size of this body in comparison to the rest of the cell. Two distinct regions are always present within each body found: a large osmiophilic region, which at high magnification is seen to consist of hexagonally packed crystalline-like fibers (Figs. 30, 31), and a clear region, the center of which contains a substructure of fibrillar/granular material of moderate electron density (Figs. 30-34). These bodies are usually seen in proximity to mitochondria (Fig. 32). Serial section analysis has shown that the region of lessened electron density appears to wind sinuously

throughout the large osmiophilic component (Figs. 33-34). These "tunnels" have been found to have an approximate diameter of 150 nm in all bodies observed.

Golgi bodies, also referred to as dictyosomes, are perinuclear in location, the cis face being in close association with the nuclear envelope (refer to Table 2 for comparison with other unicells). Figure 35 shows a typical Golgi body that has undergone intercisternal fusion, a phenomenon reported only in red algal unicells and developing red algal sporangia (Alley and Scott 1976; Garbary and Gabrielson 1990; Broadwater and Scott in press). Throughout the entire cell cycle, including mitosis, the Golgi bodies were seen actively forming large electron transparent vesicles or vacuole-like structures. These components appear to fuse with the plasma membrane (Figs. 36-38).

Glaucosphaera has a central nucleus. As shown in Figure 39, the nuclear envelope has many obvious connections with the ER. Although smooth ER (SER) is hard to locate, rough ER (RER) is seen throughout the cell. The cisternal shape of the RER appears to be dependent upon the organelles to which it is adjacent, and appears at times to radiate from the nucleus (Figs. 39-40). Another outstanding characteristic of the nuclear envelope is the numerous darkly staining nuclear pores (Figs. 14, 35-36, 39-40). Within the nucleus is found a large, densely staining nucleolus (Figs. 14, 41, 44, 45).

Mitosis:

There is little change in the overall morphology of cytoplasmic organelles during mitosis. Unless an organelle is specifically mentioned during the explanation of each mitotic stage, there is neither a change in shape nor location of that organelle.

Prophase:

As of yet, nucleus associated organelles (NAOs) in the shape of polar rings, such as have been identified in the majority of red algae investigated for mitosis, have not been found in *Glaucosphaera*. During prophase, however, presumptive microtubule-organizing centers (MTOCs) are found at opposite ends of the nucleus, establishing the division poles (Fig. 41). These MTOCs are spherical, osmiophilic bodies, averaging 0.5 μm in diameter, from which numerous microtubules emanate. Viewing both thin and thick serial sections of multiple cells have shown that these bodies are present only at each pole of the nucleus; no stages of MTOC migration to establish the poles were observed. The large number of cells in which the MTOCs were present suggests that prophase is a very long mitotic stage.

Microtubules that emanate from the MTOC in the direction of the nucleus abut and/or run parallel to the nuclear envelope, but do not enter the nucleus (Figs. 42, 43). Serial sections have shown that there are no other structures visible within the MTOC. During late prophase, the nucleolar material begins to fragment and disperse within the nucleus (Figs. 44-46). Moderately electron dense chromatin condenses as shown in figure 45, forming a "shell" around the nucleolus. Soon the MTOCs, now in close association with the nuclear envelope, begin to flatten somewhat against the nuclear surface (Fig. 46).

Prometaphase:

Prometaphase occurs when the segments of the nuclear envelope under the MTOCs become disrupted, forming a large gap at each pole. Coincident with gap formation, the MTOC continues to flatten, plugging the gap in the nuclear envelope (Figs. 47-49). All MTOC-associated microtubules now go directly into

the nucleus (Figs. 48-49). Figure 48 also shows how the polar end of each microtubule has an individual cap of MTOC material at the nuclear-cytoplasmic border. A zone of exclusion is present above the MTOC material, but serial sectioning failed to reveal any obvious structures within that area. Microtubules abut the region of the gap and radiate throughout the nucleus, some of which appear to attach to kinetochores (Fig. 49).

Metaphase:

When the metaphase plate forms, the nucleolar material is seen dispersed between the plate and the polar areas of the nucleus (Fig. 50). Serial sectioning has shown that this is a solid metaphase plate. The plate, however, appears to be limited to the center of the nucleus, as demonstrated by the large amount of electron transparent space existing between the edges of the plate and the nuclear envelope. Detailed high magnification of the kinetochores show their trilaminar morphology and attached, multiple microtubules (Fig. 51).

Anaphase:

The nucleolar material closely associates with the chromatin, possibly coating it during anaphase (Fig. 52). Anaphase A, the movement of the chromatin to the poles, appears to occur in advance of anaphase B, the migration of the poles away from one another (Figs. 53, 54). As as the nucleus elongates, the interzonal midpiece (IZM), located between the bodies of migrating chromatin-nucleolar material, achieves a relatively small diameter. The MTOC material at each pole begins to pull away from the gap and regains its previous spherical morphology. Microtubules are seen directed away from the nucleus again (Fig. 55).

Telophase:

Late anaphase-early telophase consists of an extended nucleus with a relatively short IZM (Fig. 56). Reformation of the nuclear envelope is coincident with both the disintegration of the IZM and continued reformation of the spherical MTOCs (Figs. 56-59). Vacuoles and starch grains appear between the newly formed daughter nuclei, possibly helping to maintain nuclear separation (Figs. 56-59). The cells then elongate, and obvious cleavage furrows appear during late telophase (Figs. 58-61). The nucleolar material continues to reform, taking on an interphase-like conformation (Fig. 59). The MTOC material still persists as the nuclei are further separated. The nuclei become situated in the approximate center of the forming daughter cells (Fig. 59).

Cytokinesis:

As the cleavage furrow constricts, each incipient daughter cell becomes more spherical and a dumbbell shape is formed (Figs. 58-61). The chtoplasmic region adjacent to the furrow appears unspecialized. The MTOCs soon disappear as various organelles distribute themselves between the forming daughter cells (Fig. 61). The final stages of cytokinesis were not seen using electron microscopy, however, light microscopy reveals that an extended cytoplasmic bridge may persist as the two daughter cells separate, each taking approximately equal amounts of the mucilaginous sheath with it (Fig. 62). The relative size of the young daughter cells, approximately 15 μm, is much smaller than that of a typical prophase cell, which average approximately 23 μm.

DISCUSSION

The purpose of this study was twofold. *Glaucosphaera vacuolata* is an organism that currently has no definite taxonomic affinity with any one group. As a member of the Glaucophyta, it has constantly been set aside as enigmatic, due to the large number of differences between it and the other members of this phylum. Even in the most recent treatment of the Glaucophyta, however, the placement of *Glaucosphaera* within this group has not really been questioned (Kies and Kremer 1990). An ultrastructural study of *Glaucosphaera* should help show the salient characteristics useful for comparison to groups of possible relation. Second, a study of the mitotic processes within *Glaucosphaera,* in conjunction with the vegetative characteristics, should not only demonstrate what mitotically conservative characteristics it has in common with these other groups, but would be an important addition to the growing number of mitotic studies necessary to demonstrate the validity of this process as a phylogenetic indicator (Heath 1986).

Vegetative Ultrastructure:

The Glaucophyta is composed of flagellated, colorless organisms reportedly containing modified endosymbiotic cyanobacteria within the confines of their plasma membrane (Kies and Kremer 1990). Due to the extreme rarity of the organisms of this phylum, only four members are available through culture collection centers: *Cyanophora paradoxa, Gloeochaete wittrockiana, Glaucocystis nostochinearum* and *Glaucosphaera vacuolata.*

The members of the Glaucophyta obtain their nutrition by way of inclusions termed cyanelles by Pascher (1929). Cyanelles are not true endosymbiotic cyanobacteria, but are considered to be obligate photosynthetic endosymbionts of cyanobacterial ancestry. This distinction is based on many reasons. Cyanelles have limited genetic competence, demonstrated by the large reduction of the genome of the cyanelles in *Cyanophora* compared with free living cyanobacteria, and inability to reproduce for an extended period unless within the host cell. This reduced genome is comparable in size to that of true plastids (Herdman and Stanier 1977). Cyanelles contain the pigments chlorophyll a, β-carotene, zeanthin, β-cryptoxanthin, allophycocyanin c-phycocyanin, but lack the common cyanobacterial pigments echienone and myxoxanthophyll. The pigments are located in phycobilisomes that are situated on thylakoid membranes within the cyanelles. The thylakoids appear both unstacked and concentrically arranged. Due to the similar appearance of cyanelles to the plastids contained in the Rhodophyta, Cavalier-Smith (1982) proposed placing the members of the Glaucophyceae and the Rhodophyceae into a new phylum, the Biliphyta. This taxonomic treatment, however, has never recieved support.

Coleman (1985) found three distinct patterns of DNA localization within cyanelles of the Glaucophyta. The *Cyanophora*-type consists of an irregular ring tightly surrounding a central, densely staining body. *Glaucocystis* illustrates a nucleoid in the form of a thin core of DNA running the length of the cyanelle. The third type, exhibited by both *Glaucosphaera* and red algal plastids (Scott, personal communication), is one in which multiple nucleoids are present, but not centrally confined. *Gloeochaete*, however, was not included in this study.

Although cyanelles do resemble red algal chloroplasts in both their genome size and thylakoid arrangement, there are distinct differences between the two. All cyanelles have reduced cell walls. The cyanelles of *Cyanophora* and *Glaucosystis*

were found to contain a reduced cell wall of peptidoglycan surrounding the cyanelle (Hall and Claus 1963; Schnepf and Brown 1971; Kies and Kremer 1990). Due to this peptidoglycan layer, cyanelles will not lyse when isolated from the host cells and placed into a hypo-osmotic media unless the enzyme lysozyme is added (Trench 1982). Cyanelles are also contained within vesicles of the host cell (Kies and Kremer 1990). Kremer *et al.* (1979) found that photoassimilate patterns of cyanelles differed slightly to those of the rhodophytan chloroplasts due to the lack of typical red algal heterosides, such as glycerol galactoside and mannosidoglycerate.

When viewing serially sectioned cells with the electron microscope, many tenuous connections are found to exist between the lobes of the photosynthetic organelle of *Glaucosphaera*. Detailed views of some of these connections show that thylakoid membranes may be shared between the segments, but, due to the small size of the connection, only a few to none are allowed to pass through. The low concentration of thylakoids, and therefore phycobilisomes within these connections, would explain the lack of autofluorescence of these connections. This causes the possibly single, highly lobed structure to appear as multiple, discoid units with the use of light microscopy. When cells are stored in Perfix, the photosynthetic membranes are possibly disrupted with time. This may release the phycobilin pigments, which then float freely within the envelope of the structure. These pigments could diffuse throughout the structure, possibly entering the areas within the diminutive connections. The use of autofluorescence will now show multiple connections between the segments by fluorescing the pigments within. This demonstrates that the photosynthetic organelle is possibly a single unit that is highly lobed. This organelle readily lyses upon disruption of the host cell (Trench 1982), lacking the characteristic cell wall of the cyanelles of the glaucophytes. There is no vacuole surrounding the organelle within the host, therefore making it

a cytoplasmic constituent of the cell. Due to these characteristics, and the presence of the red algal pigment R-phycocyanin, I believe that this is a single, highly-lobed plastid as proposed by McCracken *et al.* (1980). The numerous, separate cyanelles, reported by Richardson and Brown (1970), are not present.

The ultrastructure of the glaucophytan host cells are very different from that of the members of the red algae. One major difference is the presence of a flagellum. Members of the Glaucophyta possess a flagellum during at least one period of their life cycle. Due to the presence of the flagella, both basal bodies and flagellar roots are found within an apical depression in bodies of these organisms. *Glaucocystis* and *Gloeochaete* have both been found to contain four flagellar roots, while *Cyanophora* contains only two. Golgi bodies within the Glaucophyta, termed parabasal bodies, are located near basal bodies and other flagellar-associated organelles (Kies and Kremer 1990). Located directly beneath the plasma membrane of the host cells is what is referred to as either a pellicular lacunae system (Kies and Kremer 1990) or an alveolate pellicle (Cavalier-Smith 1982). This system, made of flattened vesicles, lies flatly between the plasma membrane and a layer of microtubules (Kies and Kremer 1990; Kies 1976), similar to what is seen in both the Euglenozoa and Dinozoa (Cavalier-Smith 1982).

Table 2 is a comparison of both the vegetative and mitotic characteristics of the Glaucophyta, *Glaucosphaera*, and the members of the Rhodophyta. There are many typical glaucophytan characteristics that are not present in *Glaucosphaera*. Instead of a pellicular lacunae system, a peripheral ER system is located directly underneath the plasma membrane. These systems only superficially appear similar. The peripheral ER system, also present in red algal unicells, appears continuous and is not associated with a layer of microtubules. Although not clearly visible in the fixations used in this study, micrographs from other studies (McCracken *et al.* 1980) show tubules arising out of the peripheral ER, appearing

to fuse with the plasma membrane. *Glaucosphaera* does not contain either a flagellum or any basal bodies during any part of its life cycle. This is a characteristic which is limited to the higher groups of fungi and the Rhodophyta.

Although lipid globules do occur scattered within some cyanelles of the Glaucophyta (Kies 1984), they do not appear in the typical eyespot-like arrangement commonly found within the lobes of the chloroplast of *Glaucosphaera.* Using bright-field light microscopy, these "stigmata" are perceived as small reddish-orange areas located throughout the periphery of the chloroplast lobes throughout the cell. Electron microscopic views of these areas show osmiophilic globules, with the typical arrangement of the stigmata present in red algal plastids (Deason *et al.* 1983), hexagonally packed into a plate-like configuration, usually on the side of the chloroplast lobe closest to the periphery of the cell. These stigmata are not located on a specific side, but are found throughout the circumference of the cell.

The mitochondria of *Glaucosphaera vacuolata*, although usually appearing like typical mitochondria of both the Rhodophyta and Glaucophyta, demonstrate a very unusual morphological variation in some cells. The unusual shape of these organelles consists of a flattened, stacked area in which the envelope surrounding the organelle, and possibly several elongate cristae, are easily mistaken for multiple microtubules. Thus, it has previously been mistaken as a non-emergent, flagellar axonemal component (Scott, unpublished communication). Serial sections have revealed, however, that these stacked membranes open out to reveal the characteristically flat cristae of the mitochondria found in the Rhodophyta and Glaucophyta.

An unusual, giant osmiophilic striated structure (GOSS) was found to exist within the cytoplasm of *Glaucosphaera.* This most striking freature of this body is that of the "tunnels" winding throughout it. These tunnels were of the same

diameter in all structures found, no matter what the size of the larger osmiophilic region. Mitochondria were found to have a close association with each GOSS that was found. Close observations of serial sections from multiple cells show that although a GOSS was present in many cells, it did not appear in all cells. Those that were found were usually in interphase or prophase cells. A similar structure has not been reported to exist within any protist, nor member of any other kingdom. Therefore, the presence of this body may not be helpful in making any phylogenetic decisions. Due to the unusual appearance, and thus, lack of any similarity to any previously studied structure, biochemical/cytochemical techniques would need to be employed to find out more about this unusual structure.

The cis-face, or forming-face, of Golgi bodies (dictyosomes) are usually associated with ER in eukaryotic organisms. Red algae are unusual in that they have three distinctly different Golgi body associations (Scott 1984). What is shown in almost all red algal members is a dictyosome-mitochondrial association. The members of the Porphyridiales which possess this association are *Porphyridium*, *Flintiella*, and *Rhodosorus* (Broadwater and Scott in press). The ER-dictyosome association is found only to exist in the red algal members: *Compsopogon coeruleus* (Scott and Broadwater 1989), *Rhodella maculata* and *R. violacea* (Patrone *et al.* 1991), *Smithora naiadum* (McBride and Cole 1971), *Cyanidium* (Seckback *et al.* 1991) and *Rhodochaete parvula* (Pueschel & Magne 1987) and all other observed members of the Compsopogonales (Scott, unpublished results). The third type is found only in the Porphyridiales. Occurring in both *Dixoniella grisea* and *Rhodella cyanea,* this association consists of a close opposition of the nuclear envelope with the Golgi cis-region. The Golgi bodies of *Glaucosphaera,* too, are perinuclear, showing this third type of

association, and are totally unlike the so-called parabasal bodies of the Glausophyta.

In addition, the Golgi bodies of *Glaucosphaera* were seen to have undergone intercisternal fusion, the midregions of adjacent cisternae fusing with one another. This phenomenon has been reported only in developing red algal sporangia and unicells (Broadwater and Scott in press), lending credence to the belief that red algal unicells may be reduced forms of multicellular rhodophytan reproductive cells (Garbary and Gabrielson 1990).

The various vegetative ultrastructural characteristics of *Glaucosphaera vacuolata*, such as chloroplast characteristics, Golgi body association and morphology, peripheral ER system and lack of both flagella and flagallar associated organelles strongly indicate that this unicell has a much closer relation to the Rhodophyta than to the Glaucophyta.

Mitosis:

Cyanophora paradoxa (Picket-Heaps 1972) and *Gloeochaete wittrockiana* (Kies 1976) are the only members of the Glaucophyta that have undergone extensive mitotic study. The beginning of prophase is difficult to determine, neither centrioles nor typical nuclear associated organelles (NAOs) are present within these organisms. During prophase, however, spindles consisting of microtubules form at the polar ends of the nucleus. The microtubules of these spindles radiate throughout the cell; those which emanate in the direction of the nucleus abut the nuclear membrane but do not enter. The chromatin within the nucleus condenses as the nucleolus fragments. During prometaphase, as demonstrated in *Cyanophora, Gloeochaete* and also in *Glaucocystis* (Kies and Kremer 1990), the nuclear membrane becomes distended and fragments to form an open mitotic spindle. The microtubules either attach to chromatin or go directly

through to interdigitate with the microtubules of the other spindle pole. During late anaphase-early telophase, the poles reach the extreme ends of the forming daughter cells, creating a relatively long interzonal midpiece (IZM). The spindle persists well into late telophase, possibly holding the daughter nuclei apart (Pickett-Heaps 1972), as the cleavage furrow divides the cell into two (Picket-Heaps 1972; Kies 1976; Kies and Kremer 1990).

Table 2 summarizes many of the mitotic characteristics shown by the members of the Glaucophyta, *Glaucosphaera*, and the unicellular Rhodophyta, order Porphyridiales, which have been studied thusfar. The mitotic process of *Glaucosphaera vacuolata,* unlike that of the Glaucophyta, follows a typical red algal format; however, a NAO in the form of a ring has not been found in *Glaucosphaera.* The NAO is a structure which has been found in all members of the Rhodophyta (Scott and Broadwater 1990). Its morphology usually consists of a pair of short, hollow cylinders that vary from 120 to 190 nm in diameter and in length, depending upon the species. The red alga *Batrachospermum* possesses ring-shaped NAOs, but instead of stacked, the rings have a ring-within-a-ring configuration (Scott 1983). The unicellular alga *Porphyridium purpureum,* however, has a very different NAO morphology. This NAO consists of a broad, solid granule topped by a small, flattened disk (Schornstein and Scott 1982).

The MTOC material found at the nuclear poles of *Glaucosphaera* closely resembles that of the electron dense material associated with the polar rings of the red algal unicell *Dixoniella* (Scott *et al.* 1992). All red algae show this MTOC material to some degree. The spindle formed in both *Glaucosphaera*, *Dixoniella* and the other red algal unicells would be considered type IIa according to Stewart and Mattox (1980). There are two major types of mitotic spindles formed. Type I consists of a spindle that is totally extranuclear, as seen in the dinoflagellates and hypermastigote flagellates. Type II is broken down into two categories. Type IIa,

shown in *Glaucosphaera*, consists of an intranuclear spindle that has an extranuclear origin, common to the members of the Porphyridiales, the green algae and other protozoa. IIa is also the type of spindle present in the majority of higher plants and animals. Type IIb, considered slightly more advanced than IIa (Stewart and Mattox 1980), consists of an entirely intra-nuclear spindle, seen among many fungi, Euglenids and the "higher" members of the Rhodophyta (Scott and Broadwater 1990).

During the mitotic process, trilaminar kinetochores are easily discerned in *Glaucosphaera*. Similar in appearance to those shown in several multicellular members of the Rhodophyta, the unicells studied thus far tend only to show indistinct kinetochores. As mitosis continues, both anaphase A and B movements are seen to occur in *Glaucosphaera*, as in all red algae examined for mitosis (Scott and Broadwater 1990). The red alga members *Lomentaria* (Davis and Scott 1986) and *Bossiella* (Broadwater *et al.* 1993) show a unique partitioning method of the nucleolar material, which is especially obvious during anaphase B. Nucleolar material attaches to and trails the migrating chromatin. The nucleolar material of *Glaucosphaera,* however, completely surrounds the chromatin by mid to late anaphase B, causing the two to travel simultaneously. This is similar to the nucleolar behavior in some green algal cells, in which the nucleolar material coats the chromosomes and both thus travel simultaneously (Picket-Heaps 1970).

A relatively short IZM is formed during late anaphase, similar to that of *Rhodella violacea, R. maculata*, and *Dixoniella grisea*, which are in the family Porphyridaceae (Broadwater and Scott in press). *Flintiella* is the only member of the other family of the Porphyridiales, the Phragmonemataceae, which has undergone a mitotic study. This organism has a very long IZM in which the incipient daughter nuclei reach the extreme ends of the cell. Vacuoles and other organelles were seen to appear between the nuclei shortly after the IZM dissolved

and the daughter nuclei reformed. This same pattern of nuclear behavior is also characteristic of *Porphyridium* (Schornstein and Scott 1982).

The nuclear envelope of *Glaucosphaera* persists throughout the mitotic cycle, except for a gap at each pole. This gap, however, is not open to the cytosol of the cell. The MTOC settles upon the nuclear envelope and flattens, closing the gap as it is created. This is a phenomenon that characterizes all members of the Rhodophyta with polar gaps. There are two general types of mitosis shown within the Rhodophyta (Broadwater *et al.* 1993). In the majority of multicellular species, the nuclear envelope, which is surrounded either totally (*Polysiphonia*-like) or partially (*Lomentaria*-like) with perinuclear ER (PER), develops many small openings at its poles during prometaphase. This type, typical of the morphologically more advanced algae, is termed the "polar fenestrations" (PF) type of mitosis (Broadwater *et al.* 1993). The "polar gap" (PG) type occurs in all unicellular and select multicellular species. Three variations of this include: *Batrachospermum*-type, *Flintiella*-type, and *Porphyridium*-type (Scott and Broadwater 1990). The *Batrachospermum*-type mitosis is indicated by a nucleus, partially surrounded by PER, which forms two, deeply penetrating microtubule-filled pockets at the poles before gap formation. Mitosis in *Flintiella* is identical to that of *Batrachospermum*, except there is no PER present. The *Porphyridium*-type mitosis consists of a PER free nucleus in which only one shallow pocket is formed within each polar area before a small gap is formed. Although prometaphase pockets were not seen, mitosis in *Glaucosphaera,* most closely resembles the *Porphyridium*-type of PG mitosis. This type of mitosis is also seen in the red algal unicells *Dixoniella, Rhodella violacea* and *R. maculata.*

Glaucosphaera vacuolata has both vegetative and mitotic characteristics similar to those of the unicellular red algae comprising the order Porphyridiales. *Glaucosphaera* demonstrates all of the characteristics used to define the members

of the Rhodophyta. The only obvious differences between it and the present members of the Rhodophyta are the lack of a typical NAO, presence of the GOSS within the cytoplasm, and the nucleolar behavior during mitosis. Due to an obvious lack of common characteristics with any of the members of the Glaucophyta, in which it is presently classified, I recommend that it be reclassified and placed within the Porphyridiales. I believe that the differences between *Glaucosphaera* and the members of the Porphyridiales fit well into the variation already present within the order. Although, both ultrastructurally and mitotically, *Glaucosphaera* most closely matches *Dixoniella grisea,* a member of the Porphyridiaceae, it should be placed in the family Phragmonemataceae. This is due to the present taxonomic convention of segregating unicellular red algae according to the presence or absence of a pyrenoid.

BIBLIOGRAPHY

Alley, C.D. and J.L. Scott (1976) Unusual dictyosome morphology and vesicle formation in tetrasporangia of the marine red alga *Polysiphonia denudata. J. Ultrastruct. Res.* 58:289-298.

Broadwater, S.T. and J.L. Scott (in press) Ultrastructure of unicellular red algae. In: *Enigmatic Algae and Evolutionary Pathways* (Seckback, J. ed.). Kluwer Scientific Academic Publishers.

Broadwater, S., J. Scott, D. Field, B. Saunders and J. Thomas (1993) An ultrastructural study of cell division in the coralline red alga *Bossiella orbigniana. Can. J. Bot.* 71:434-446.

Cavalier-Smith, T. (1982) The origin of plastids. *J. Linn. Soc.* 17:289-306.

Chapman, R.L. and N.J. Lang (1973) Virus-like particles and nuclear inclusions in the red alga *Porphyridium purpureum* (Bory) Drew Et Ross. *J. Phycol.* 9:117-122.

Coleman, A.W. (1985) Cyanophyte and cyanelle DNA: A search for the origins of plastids. *J. Phycol.* 21:371-379.

Davis, E. and J. Scott (1986) Ultrastructure of cell division in the marine red alga *Lomentaria baileyana.* Protoplasma. 131:1-10.

Deason, T.R., G.L. Butler and C. Rhyne (1983) *Rhodella reticulata* SP. NOV., a new coccoid rhodophytan alga (Porphyridiales). *J. Phycol.* 19:104-111.

Gabrielson, P.W. and D.J. Garbary (1986) Systematics of red algae (Rhodophyta). *CRC Crit. Rev. Plant Sci.* 3:325-366.

Gabrielson, P.W. and D.J. Garbary (1987) A cladistic analysis of Rhodophyta: florideophycidean orders. *Br. Phycol. J.* 22:125-138.

Garbary, D.J. and P.W. Gabrielson (1990) Taxonomy and evolution. In: *Biology of the Red Algae* (K.M. Cole and R.G. Sheath, eds.). pp. 477-497. Cambridge University Press, Cambridge.

Garbary, D.J., G.I. Hanson and R.F. Scagel (1980) A revised classification of the Bangiophyceae (Rhodophyta). *Nova Hedw.* 33:145-166.

Goff, L.J. and A.W. Coleman (1984) Elucidation of fertilization and development in a red alga by quantitative DNA microspectrofluorometry. *Devel. Bio.* 102:173-194.

Goff, L.J. and A.W. Coleman (1990) DNA: microspectrofluorometric studies. In: *Biology of the Red Algae* (K.M. Cole and R.G. Sheath, eds.). pp. 43-71. Cambridge University Press, Cambridge.

Hall, W.T. and G. Claus (1963) Ultrastructural studies on the blue-green algal symbiont in *Cyanophora paradoxa* Korschikoff. *J. Cell Biol.* 19:551-563.

Heath, B. (1986) Nuclear division: a marker for protist phylogeny? *Progr. Protist.* 1:115-162.

Herdman, M. and R. Stanier (1977) The cyanelle: chloroplast or endosymbiotic prokaryote? *FEMS Letters.* 1:7-12

Kies, L. (1976) Untersuchungen zur feinstruktur und taxonomischen einordnung von *Gloeochaete wittrockiana*, einer apoplastidalen capsalen alge mit blaugrunen endosymbioten (Cyanellen). *Protoplasma.* 87:419-446.

Kies, L. (1984) Cytological aspects of blue-green algal endosymbiosis. In: *Compartments in Algal Cells and Their Interaction* (W. Weissner, D. Robinson, and R.C. Star, eds.). pp. 191-199. Springer-Verlag: Berlin-Heildelberg.

Kies, L. and B.P. Kremer (1990) Phylum Glaucocystophyta. In: *Handbook of Protoctista* (eds. L. Margulis, J.O. Corliss, M. Melkonian, D.J. Chapman) pp.152-166. Jones and Bartlett Pub.: Boston.

Korschikoff, A.A. (1930) *Glaucosphaera vacuolata*, a new member of the Glaucophyceae. *Arch. Protistenk.* 70:217-222.

Kremer, B.P., L. Kies and A Rostami-Rabet (1979) Photosynthetic performance of cyanelles in the endocyanomes *Cyanophora*, *Glaucosphaera*, *Gloeochaete*, and *Glaucocystis*. *Z. Pflanzenphysiol. Bd.* 92 S 303-317.

Lamouroux, J.V.F. (1813) Essai sur les genres de la famille de thalassiophytes, non articulées. *Ann. Mus. Natl. Hist. Nat., Paris.* 20:115-139, 267-293.

Lee, R.E. (1980) *Phycology.* Cambridge: Cambridge University Press.

McBride, D.L. and K. Cole (1971) Electron microscopic observations on the differentiation and release of monospores in the marine red alga *Smithora naiadum*. *Phycologia.* 10:49-61

McCracken, D.A., M.J. Nadakavukaren and J.R. Cain (1980) A biochemical and ultrastructural evaluation of the taxonomic position of *Glaucosphaera vacuolata* Korsch. *New. Phytol.* 86:39-44.

Pascher, A. (1929) Studien über Symbiosen. I. Über einige endosymbiosen von blaualgen en einzellern. *Jahrb. Wiss. Bot.* 71:386-462.

Patrone, L.M., S.T. Broadwater and J.L. Scott (1991) Ultrastructure of vegetative and dividing cells of the unicellular red algae *Rhodella violacea* and *Rhodella maculata*. *J. Phycol.* 27:742-753.

Picciolo, G.L. and D.S. Kaplan (1984) Reduction of fading of fluorescent reaction product for microphotomertic quantitation. *Adv. App. Micro.* 30:197-209.

Pickett-Heaps, J.D. (1970) The behavior of the nucleolus during mitosis in plants. *Cytobios.* 6:69-78.

Pickett-Heaps, J. (1972) Cell division in *Cyanophora paradoxa*. *New Phytol.* 71:561-567.

Pueschel, C.M. (1990) Cell Structure. In: *Biology of the Red Algae* (K.M. Cole and R.G. Sheath, eds.). pp. 7-41. Cambridge University Press, Cambridge.

Pueschel, C.M. and F. Magne (1987) Pit plugs an other ultrastructural features of systematic value in *Rhodochaere parvula* (Rhodophyta, Rhodochaetales). *Cryptogam. Algol.* 8:201-209.

Richardson, F.L. and T.E. Brown (1970) *Glaucosphaera vacuolata*, its ultrastructure and physiology. *J. Phycol.* 6:165-171.

Schnepf, E. and R.M. Brown (1971) On relationships between endosymbiosis and the origins of plastids and mitochondria. In: *Origin and Continuity of Cell Organelles* (Reinert, J., H. Ursprung, eds.). pp. 299-322. Springer-Verlag: Heidelberg, Berlin.

Schornstein, K.L. and J. Scott (1982) Ultrastructure of cell division in the unicellular red alga *Porphyridium purpureum*. *Can. J. Bot.* 60:85-97.

Scott, J. (1983) Mitosis in the freshwater red alga *Batrachospermum ectocarpum*. *Protoplasma*. 118:56-70.

Scott, J. (1984) Electron microscopic contributions to red algal phylogeny. J. Phycol. 20, suppl.:6

Scott, J. (1986) Ultrastructure of cell division in the unicellular red alga *Flintiella sanguinaria*. *Can. J. Bot.* 64:516-524.

Scott, J., C. Bosco, K. Schornstein and J. Thomas (1980) Ultrastructure of cell division and reproductive differentiation of male plants in the Florideophyceae (Rhodophyta): cell division in *Polysiphonia*. *J. Phycol.* 16:507-524.

Scott, J. and S. Broadwater (1989) Ultrastructure of vegetative organization and cell division in the frestwater red alga *Compsopogon. Protoplasma.* 152:112-122.

Scott, J. and S. Broadwater (1990) Cell division. In: *Biology of the Red Algae* (K.M. Cole and R.G. Sheath, eds.). pp. 123-145. Cambridge University Press: Cambridge.

Scott, J., S. Broadwater, B. Saunders, J. Thomas and P. Gabrielson (1992) Ultrastructure of vegetative organization and cell division in the unicellular red alga *Dixoniella grisea* Gen. Nov. (Rhodophyta) and a consideration of the Genus *Rhodella. J. Phycol.* 28:649-660.

Seckback, J., I.S. Hammerman and J. Hanania (1981) Ultrastructural studies of *Cyanidium caldarium*: contribution to phylogenesis. *Ann N.Y. Acad. Sci.* 361:409-425.

Stewart, K.D. and K. Mattox (1980) Phylogeny of phytoflagellates. In: *Phytoflagellates* (Cox, E.R ed.). pp. 433-462. North Holland Elsevier: N.Y.

Trench, R.K. (1982) Physiology, biochemistry, and ultrastructure of cyanellae. In: *Progress in Phycological Research.* Vol 1 (Round, F.E., D.J. Chapman, eds.). pp. 257-288. Elsevier Biomedical Press: N.Y.

Table 1

Mitotic Peak Study

Time	Sample Number	Sample Size	Number Dividing	Percent Dividing
8:00	1	504	0	0.00
8:20	2	501	4	0.80
8:40	3	505	6	1.19
9:00	4	505	7	1.39
9:20	5	504	4	0.79
9:40	6	502	6	1.19
10:00	7	505	8	1.58
10:20	8	509	7	1.38
10:40	9	504	9	1.79
11:00	10	501	2	0.40
11:20	11	506	8	1.59
11:40	12	503	6	1.19
12:00	13	514	6	1.17
12:20	14	503	5	0.99
12:40	15	501	6	1.20
13:00	16	504	7	1.39
13:20	17	509	6	1.18
13:40	18	509	4	0.79
14:00	19	507	3	0.59
14:20	20	510	3	0.59
14:40	21	505	2	0.40
15:00	22	509	1	0.20
15:20	23	500	3	0.60
15:40	24	500	1	0.20
16:00	25	503	2	0.40
16:20	26	507	1	0.20
16:40	27	502	0	0.00
17:00	28	505	0	0.00
17:20	29	-	-	-
17:40	30	-	-	-
18:00	31	504	0	0.00
18:20	32	-	-	-
18:40	33	-	-	-
19:00	34	502	0	0.00
19:20	35	-	-	-
19:40	36	-	-	-
20:00	37	502	0	0.00
20:20	38	-	-	-
20:40	39	-	-	-
21:00	40	511	0	0.00
21:20	41	-	-	-
21:40	42	-	-	-
22:00	43	518	0	0.00
22:20	44	-	-	-
22:40	45	-	-	-
23:00	46	507	0	0.00
23:20	47	-	-	-
23:40	48	-	-	-
0:00	49	502	0	0.00
0:20	50	-	-	-
0:40	51	-	-	-
1:00	52	507	0	0.00
1:20	53	-	-	-
1:40	54	-	-	-
2:00	55	509	0	0.00
2:20	56	-	-	-
2:40	57	-	-	-
3:00	58	504	0	0.00
3:20	59	-	-	-
3:40	60	503	0	0.00
4:00	61	500	0	0.00
4:20	62	501	0	0.00
4:40	63	507	0	0.00
5:00	64	500	0	0.00
5:20	65	501	1	0.20
5:40	66	503	3	0.60
6:00	67	501	3	0.60
6:20	68	505	3	0.59
6:40	69	504	3	0.59
7:00	70	504	6	1.19
720	71	504	12	2.38
7:40	72	500	13	2.60

The symbol - denotes that cells were not counted. Bold numerals indicate the dark period.

Table 2

Name	Size (in μm)	Flagella	PER	Chloroplast Shape	Peripheral Thylakoid	Pyrenoid	Golgi Body Association	Nuclear Location	NAO Type	Metaphase Pole	Kinetochore Morphology	IZM Length
Glaucophyta: various species	Varies with Species	Yes	No	Cyanelles, cell walls present	Yes	No	Para-basal	Various Locations	None	Open Mitotic Spindle	Not visible	Long
Glaucosphaera vacuolata	17-26	No	Yes	Single, Highly Lobbed	Yes	No	Nuclear	Central	None	Gap	Distinct Trilaminar Structure	Short
Flintiella sanguinaria	6-14	No	Yes	Single, Peripheral	No	No	ER-Mitochondria	Eccentric	Ring	Gap	Small Indistinct Structure	Long
Dixoniella grisea	8-32	No	Yes	Stellate, Highly Lobbed	Yes	Eccentric with Thylakoids	Nuclear	Eccentric	Ring	Gap	Small Indistinct Structure	Short
Rhodella violacea	8-30	No	Yes	Stellate, Highly Lobbed	No	Eccentric	ER	Eccentric	Ring	Gap	Small Indistinct Structure	Short
Rhodella maculata	7-24	No	Yes	Stellate, Highly Lobbed	No	Eccentric	ER	Eccentric	Ring	Gap	Small Indistinct Structure	Short
Rhodella cyanea	22-40	No	Yes	Radial, Centrally Fused	No	Peri-nuclear	Nuclear	Central	?	?	?	?
Porphyridium purpureum	5-13	No	Yes	Stellate	No	Central with Thylakoids	ER-Mitochondria	Peripheral	Proximal Disk and Distal Ring	Gap	Small Indistinct Structure	Long
Porphyridium aeruginium	5-13	No	Yes	Stellate	No	Central with Thylakoids	ER-Mitochondria	Peripheral	?	?	?	?
Rhodosorus marinus	5-15	No	Yes	Peripheral Cup-Shaped	No	Peripheral with Thylakoids	ER-Mitochondria	Peripheral	Ring	?	?	?

Figure 1

Population Growth Study

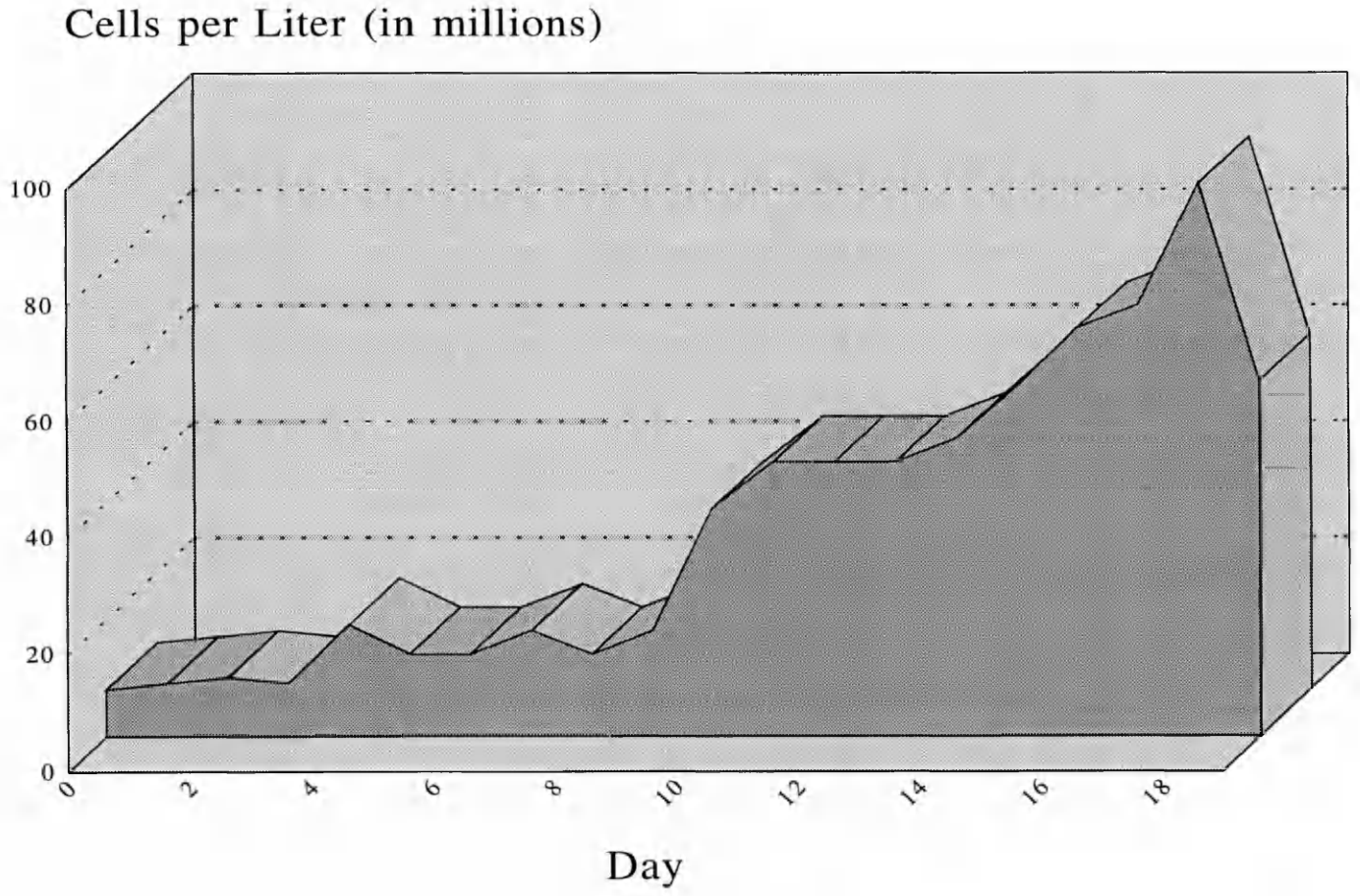

Figure 2

Mitotic Peak Study

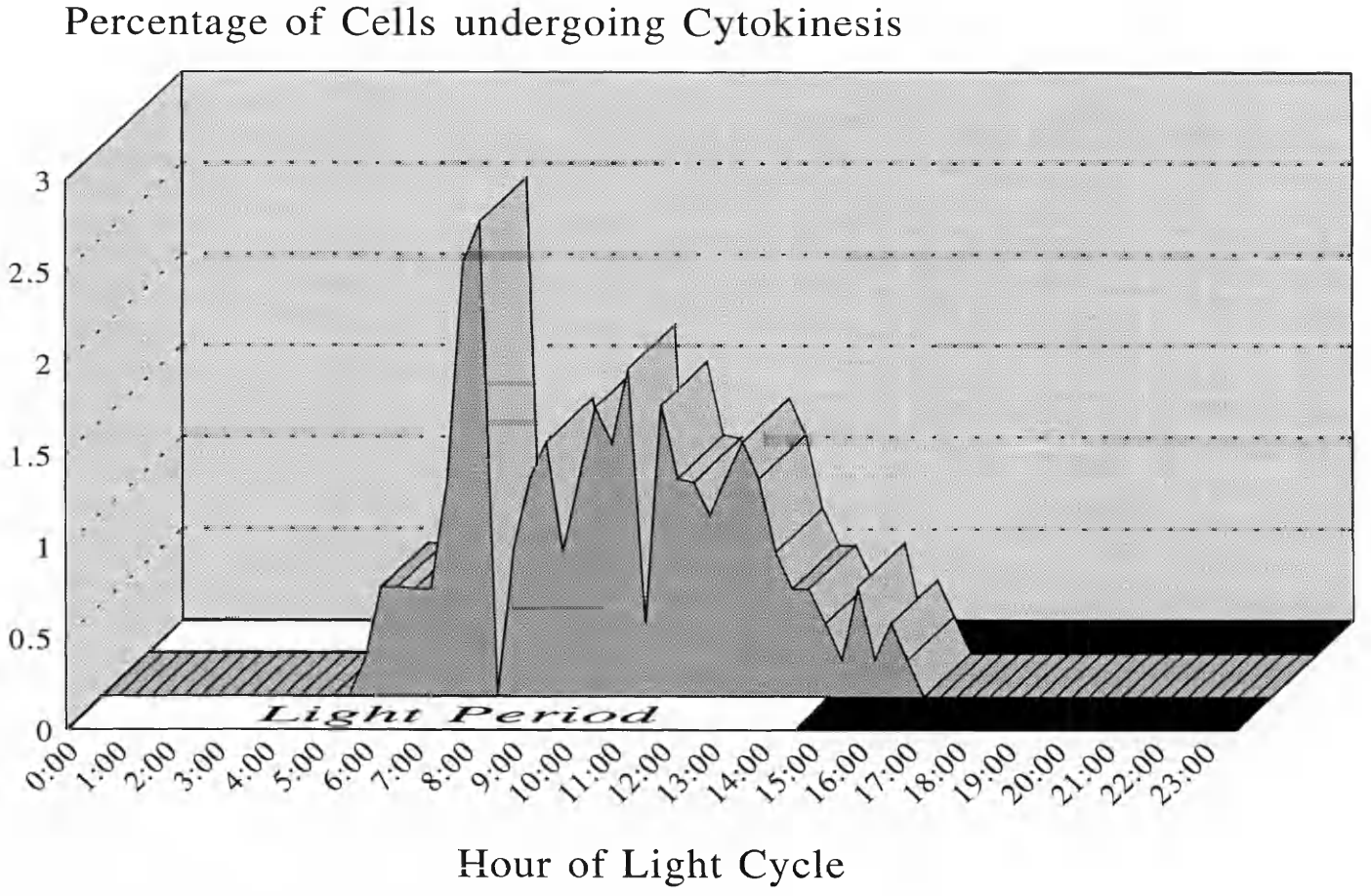

Fig. 3. Nomarski DIC of concentrated cells. Cells show an even hexagonal spacing pattern. x 750.

Fig. 4. Nomarski DIC and India Ink. The mucilaginous sheaths of the cells abut one another, not allowing cells to come into contact . x 1,300

Fig. 5. Nomarski DIC and India Ink. High magnification view showing detail of cell. x 2,800

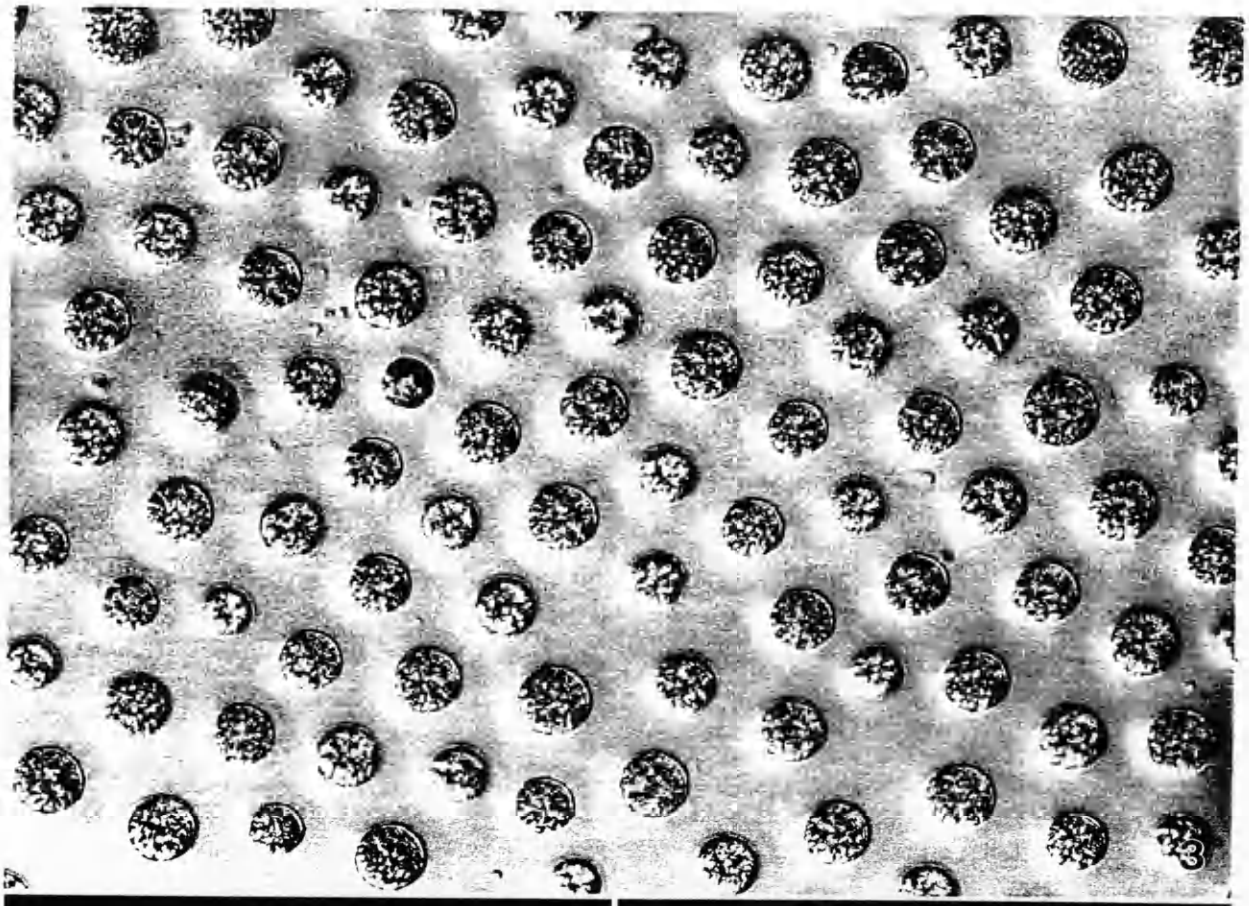

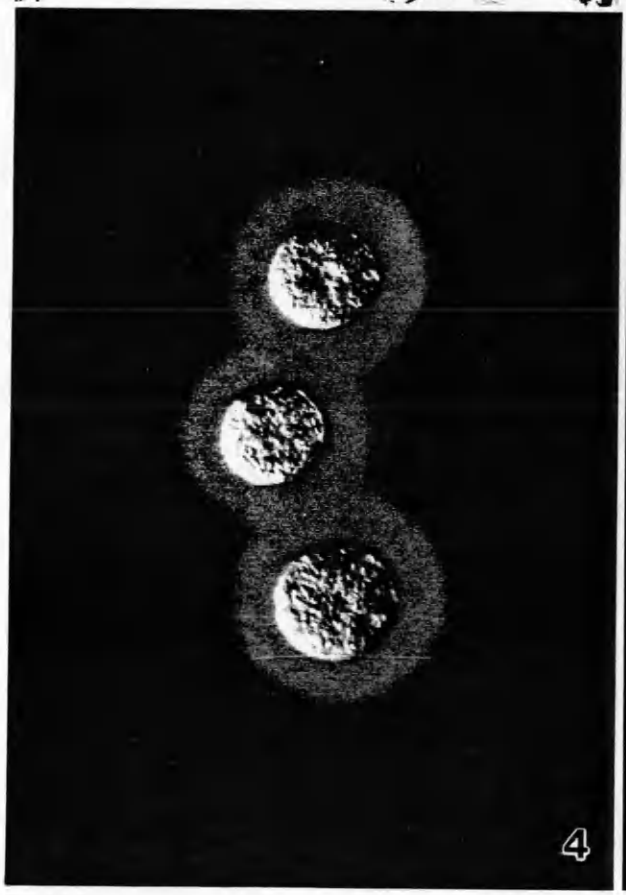

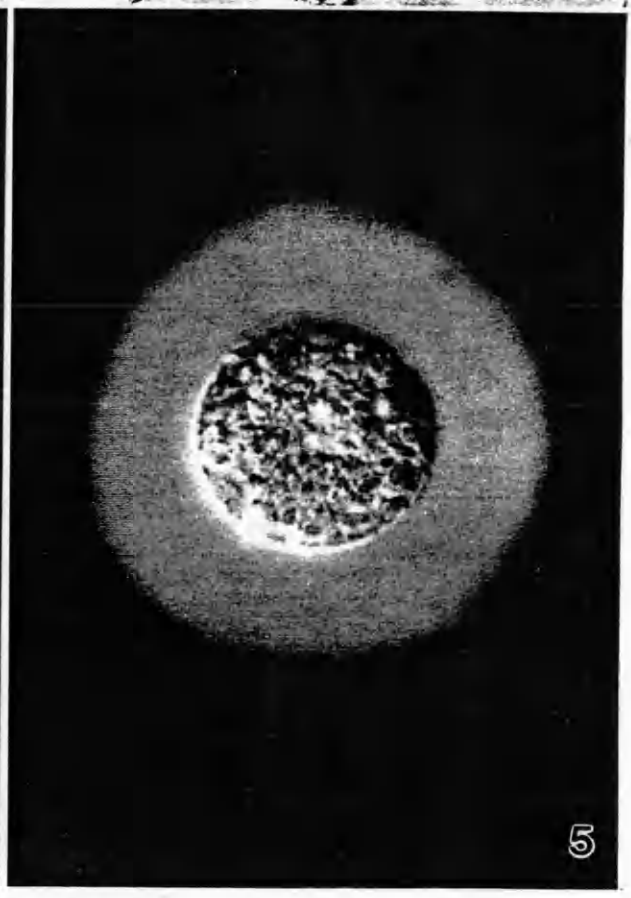

Fig. 6. Fluorescence. High magnification of normal cell demonstrating autofluorescence. x 4,000.

Fig. 7. Fluorescence with DAPI. Scattered regions of localized DNA appear as brightly staining points dispersed throughout plastid. x 3,200.

Fig. 8. Fluorescence with DAPI. Cell demonstrating interphase-prophase condition of chromatin. x 2,500.

Fig. 9. Fluorescence with DAPI. Metaphase. x 2,500.

Fig. 10. Fluorescence with DAPI. Early anaphase. x 2,500.

Fig. 11. Fluorescence with DAPI. Late anaphase. x 2,500.

Fig. 12. Fluorescence with DAPI. Telophase. x 2,500.

Fig. 13. Fluorescence with DAPI. Cytokinesis. x 2,500.

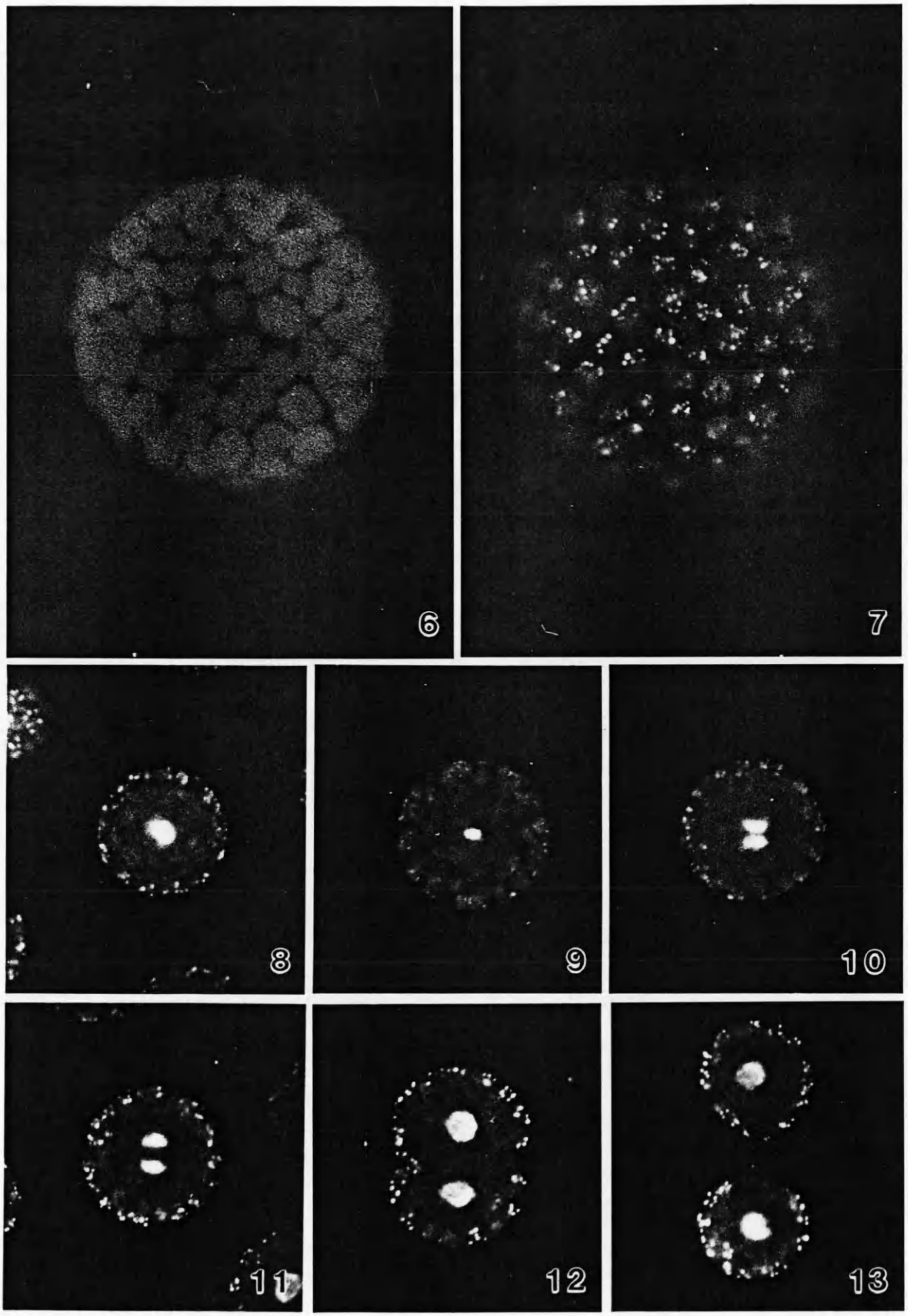
6
7
8
9
10
11
12
13

Fig. 14. Whole cell view of *Glaucosphaera*. Medial section of vegetative cell, showing chloroplast (C), Golgi bodies (G), mitochondria (M), nucleolus (N), nucleus (Nu), cytoplasmic starch deposits (S), and vacuoles (V). x 12,200.

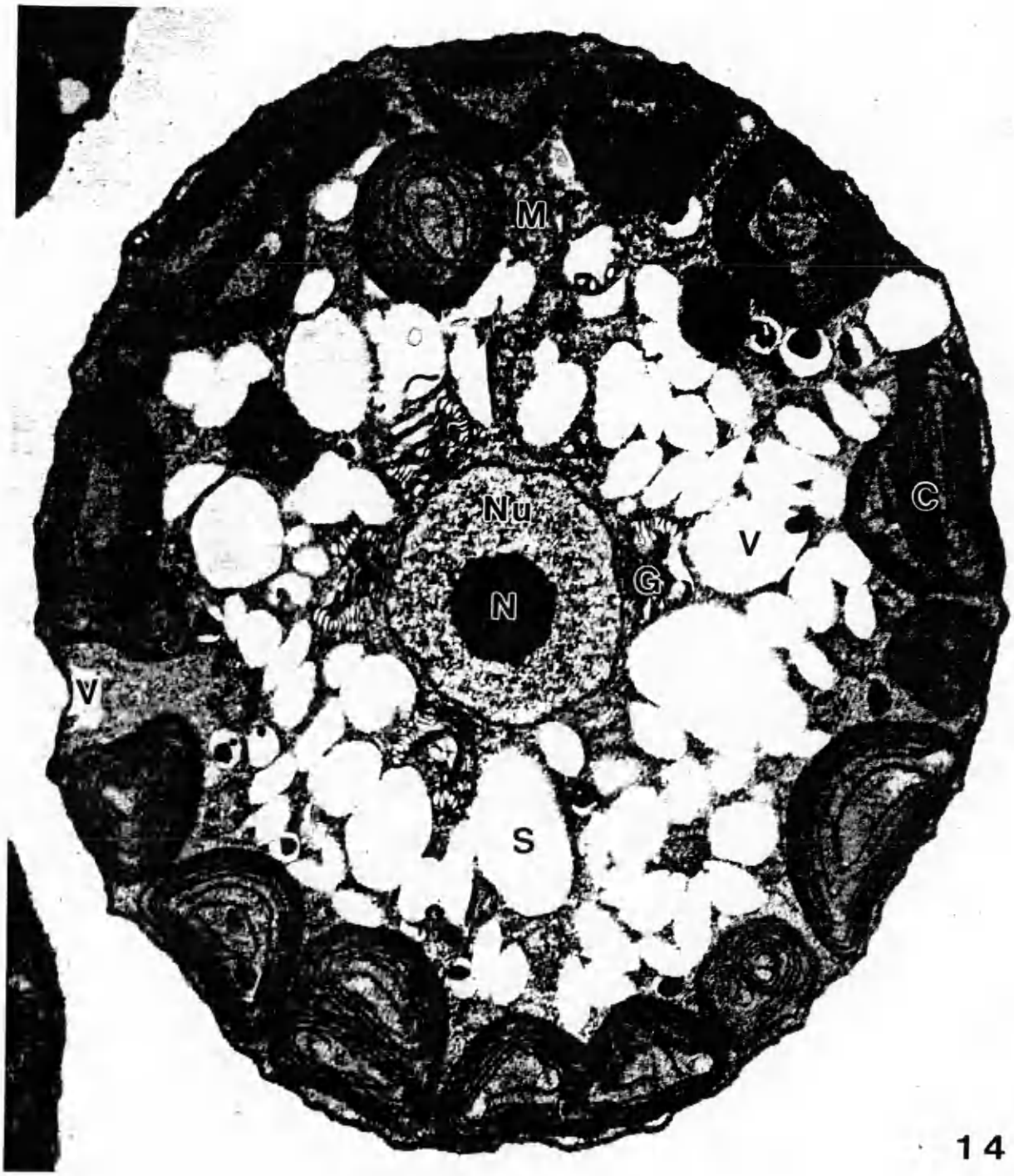

14

Fig. 15. Viral particles. These particles were usually found at the cell's periphery (arrowheads). x 12,200.

Fig. 16. High magnification view of viral particles. x 66,000.

Fig. 17. Eyespots. Glancing sections of cells often reveal a hexagonally arrangement of osmiophilic globules within the matrix of the chloroplast. x 90,000.

Fig. 18. Globules of eyespots were arranged in a single layer against the plastid envelope, usually close to the periphery of the cell. x 70,000.

Fig. 19. Phycobilisomes. These structures appear similar to that of closely stacked coins standing on their edges upon the thylakoid membrane. Note rectangular shape when sectioned from above (arrowhead). x 40,500.

Fig. 20. View of phycobilisomes showing coin-like morphology. Note the single, unstacked thylakoids upon which they are located. x 125,700.

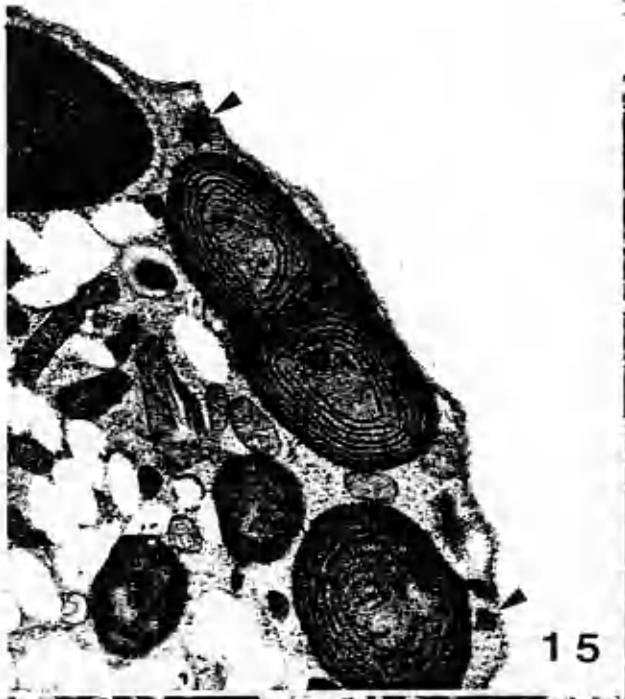

15

16

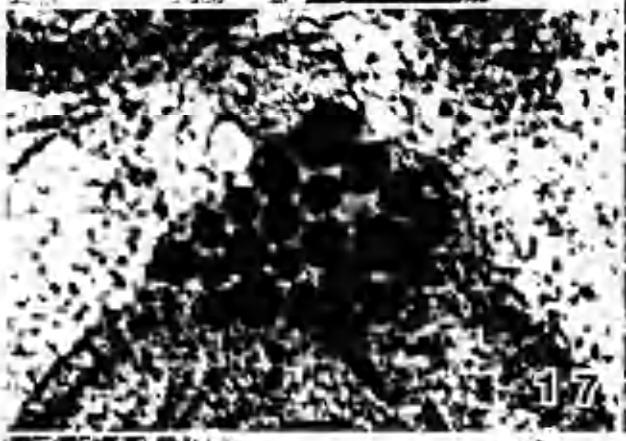

17

18

19

20

Fig. 21. Fluorescence. Cell showing multiple connections between chloroplast lobes through autofluorescence. x 1,700.

Fig. 22. Chloroplast connections spanning across the entire cell shown in a glancing section. x 8,700.

Fig. 23. Connection located at the periphery of the cell. Note the presence of a peripheral endoplasmic recticulum system (arrowheads). x 36,000.

Fig. 24. Connection between lobes of the chloroplast through which thylakoid membranes pass. x 27,300.

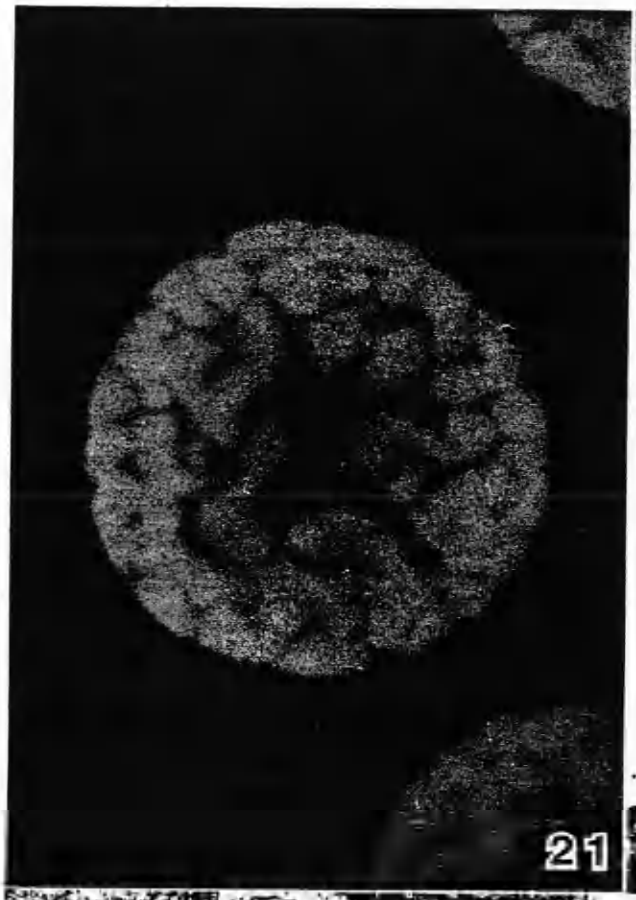
21

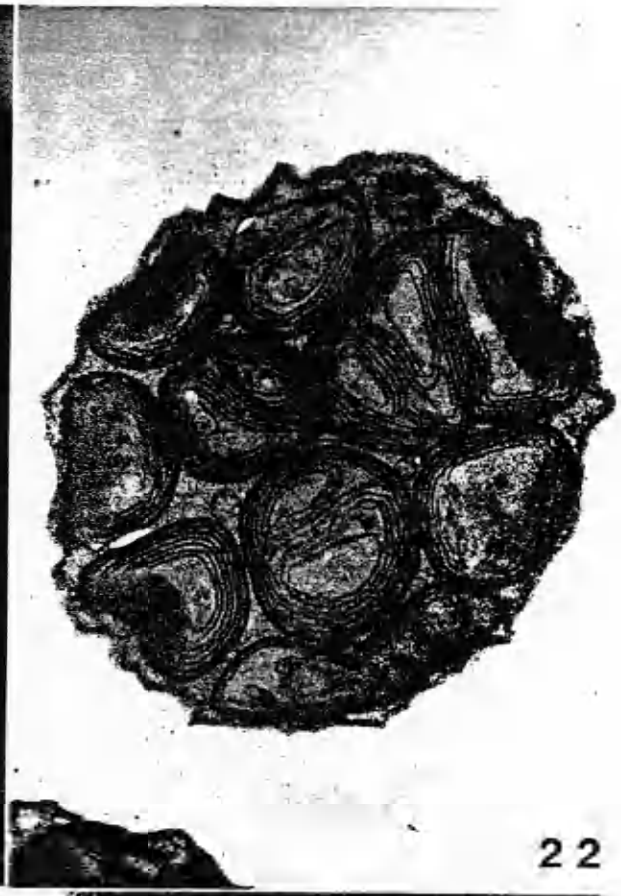
22

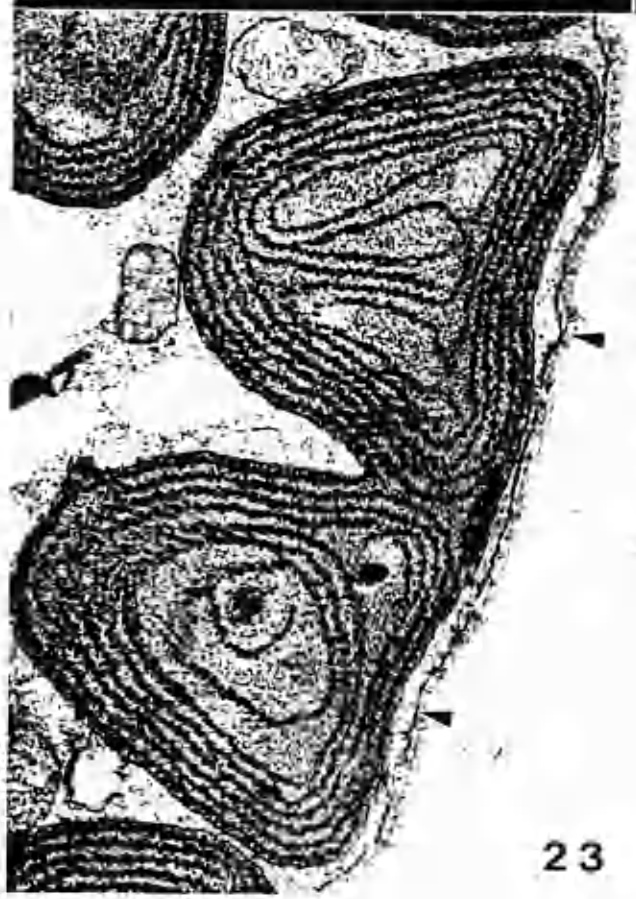
23

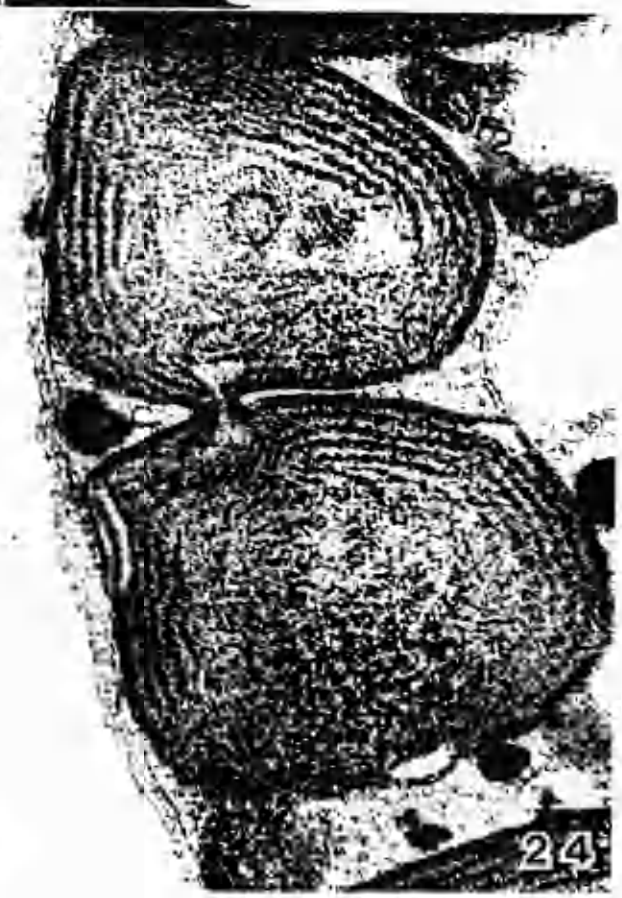
24

Fig. 25. Mitochondria. The mitochondria (M) sometimes posses a flattened region (arrowheads). x 18,000.

Fig. 26. High magnification of the flattened region reveals typical flattened cristae within (arrowhead). x 40,300.

Figs. 27-28. Serial sections revealing that the stacked tubule-like structure appears to be a modification of the envelope surrounding the mitochondria (arrowheads). x 27,300.

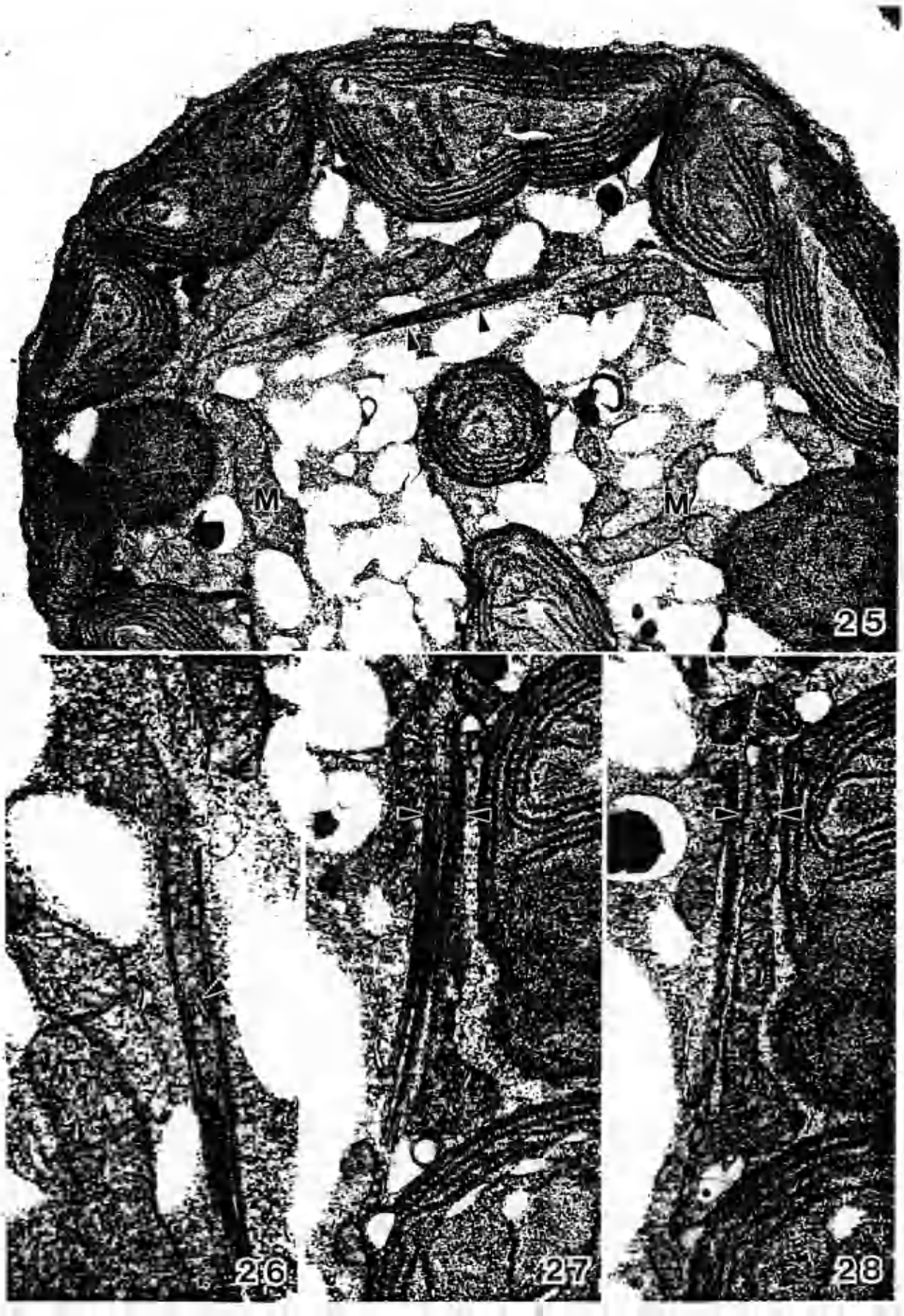

Fig. 29. Whole cell view showing relative size of a giant osmiophilic striated structure (GOSS) in the periphery of the cell (arrowhead). x 6,000.

Fig. 30. High magnification of GOSS showing crystalline-like substructure of osmiophilic region (arrowheads). Note the close proximity of mitochondria (M). x 42,000.

Fig. 31. A very ordered spacing pattern occurs between each region of the GOSS. Note the electron free regions (arrows), moderately electron dense regions (arrowhead) and a "honeycombed" view of the crystalline-like substructure within the osmiophilic region (∗). x 42,000.

Fig. 32. Mitochondria (M) are seen to have an association with the GOSS. x 62,900.

Figs. 33-34. Skipped serial sections show that the GOSS has a more complex morphology than a mere stacking of different regions. x 42,000.

29

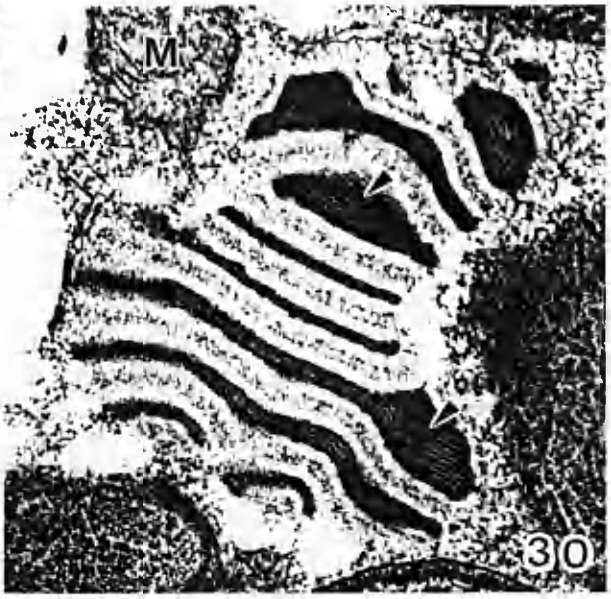

30

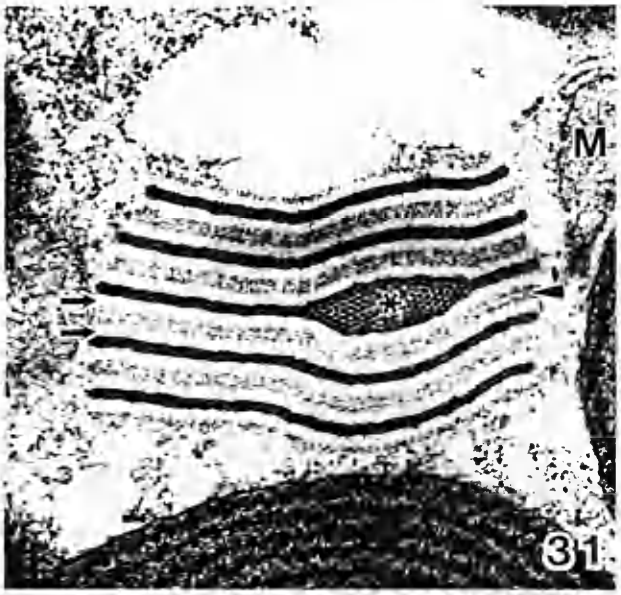

31

32

33

34

Fig. 35. Perinuclear Golgi body showing intercisternal fusion. Note the cytoplasmic starch deposits (S) which lack the limiting membrane present around vacuoles (V). Arrows indicate location of the nuclear envelope. x 42,000.

Fig. 36. Golgi body actively forming vesicle (V). x 38,000.

Fig. 37. Golgi-derived vesicles (V) are secreted at the periphery located directly above Golgi body. x 21,000.

Fig. 38. An in-pocketing of the plasma membrane is usually seen above vacuoles (V) at the periphery of the cell. x 21,000.

Fig. 39. Rough endoplasmic recticulum (RER) is often seen connected to the nuclear envelope (arrowhead). Note the presence of densly staining nuclear pores in the envelope (arrow). x 56,300.

Fig. 40. Long, straight cisternae of RER (arrowheads) often radiate through the cytoplasm from the nuclear envelope. x 21,000.

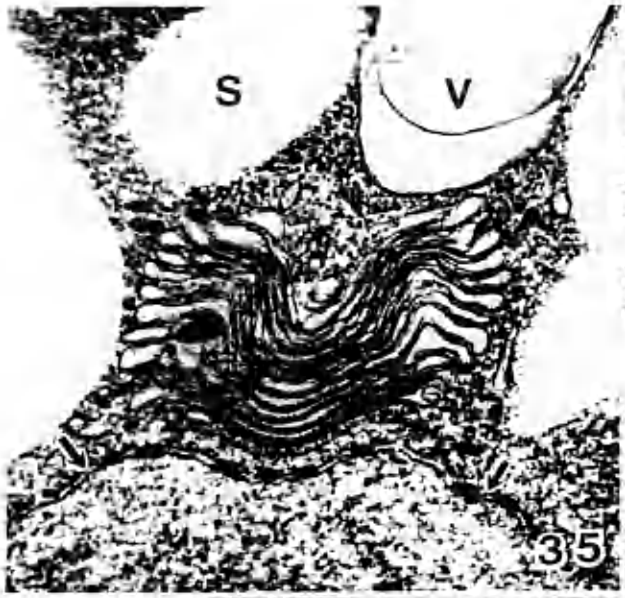
S
V
35


V
36

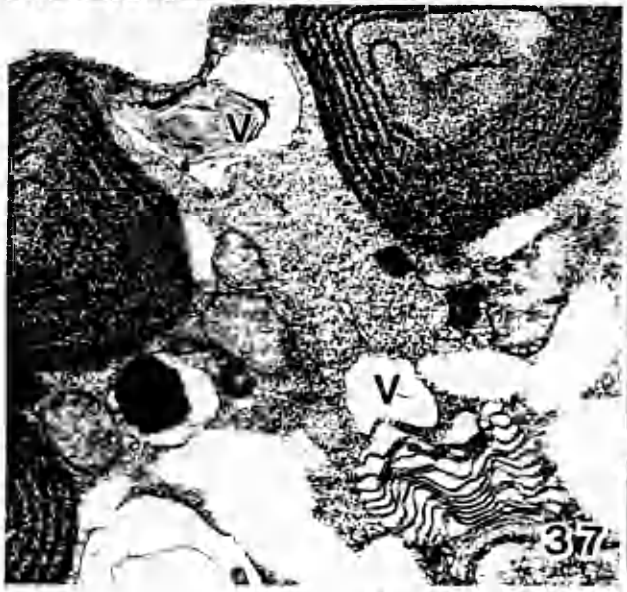
V
V
37

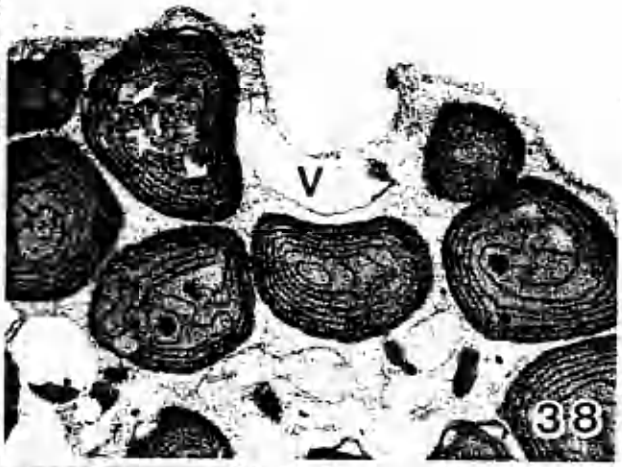
V
38


39

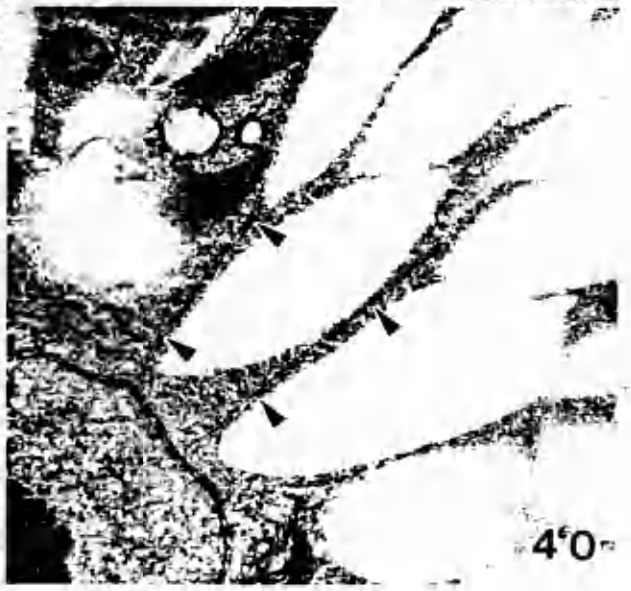
40

Fig. 41. Prophase. Two poles are seen, defined by spheres of microtubule organizing centers (MTOCs). Note the dense nucleolus (N) in the center of the nucleus. x 12,200.

Fig. 42. High magnification of top pole, from previous micrograph, showing multiple microtubules emanating from within. x 38,000.

Fig. 43. Microtubules (arrowheads) are the only distinguishable structures within the spheres of MTOC material. x 90,000.

Fig. 44. The nucleolus (N) fragments during prophase. x 7,800.

Fig. 45. Chromatin condenses to form a shell around fragmented nucleolus (N). x 12,200.

Fig. 46. MTOC material begins to flatten against the nuclear membrane. x 12,200.

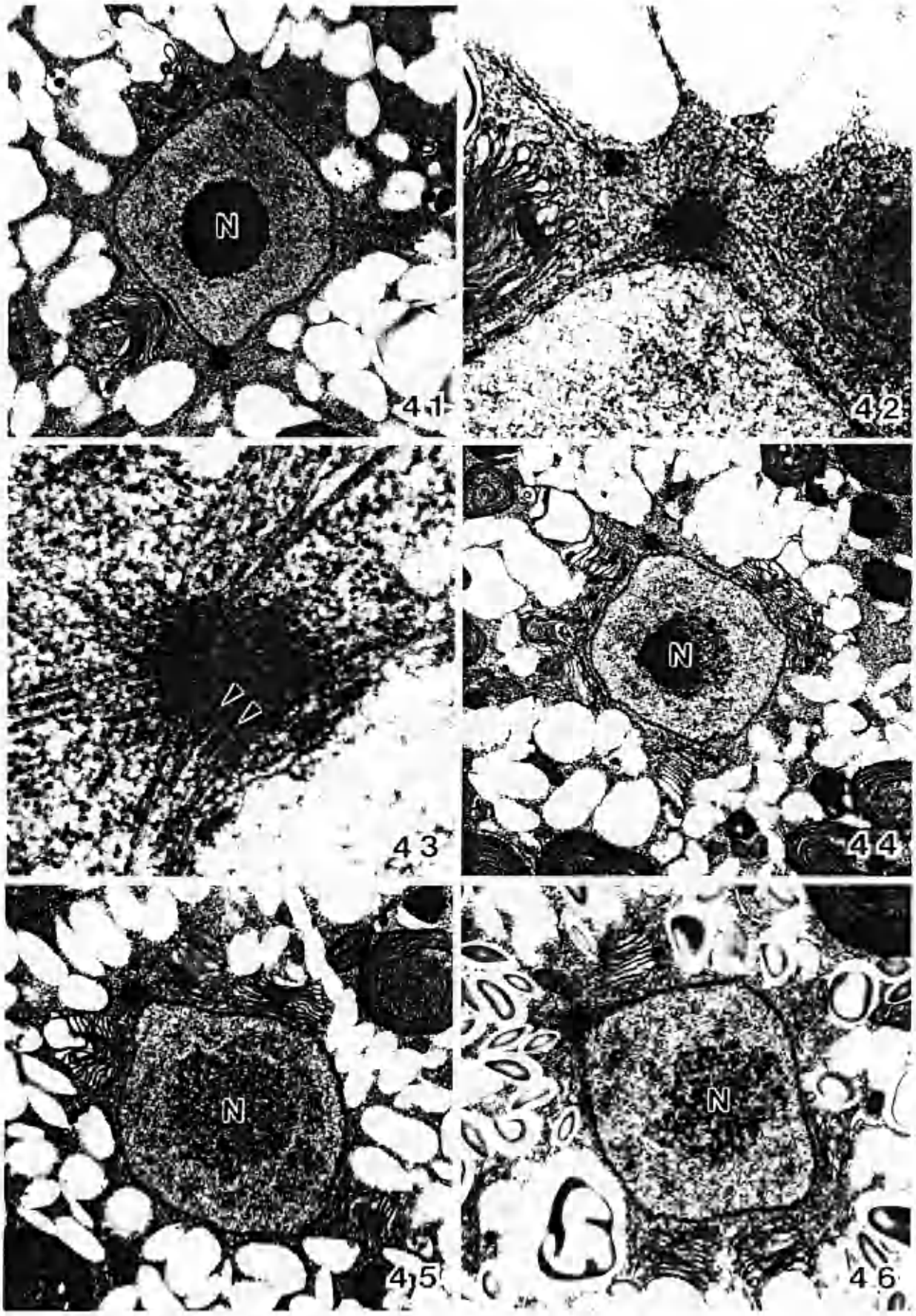
N
4 1
4 2
4 3
N
4 4
N
4 5
N
4 6

Fig. 47. The nuclear envelope (arrowheads) forms a gap beneath the flattened MTOC. Microtubules are now seen within the nucleus. x 37,200.

Fig. 48. High magnification of pole shows a gap in nuclear envelope (arrowheads) which is plugged with the MTOC material. No discernible structure is visible in zone of exclusion located above flattened MTOC material. x 59,600.

Fig. 49. Microtubules run through nucleolar material (N) and attach to kinetochores on the chromatin (Ch). x 21,000.

Fig. 50. A typical metaphase plate forms in the center of the nucleus. x 12,200.

Fig. 51. High magnification of metaphase plate shows distinct trilaminar kinetochores (arrowheads). Note the presence of an intact nuclear envelope (arrows). x 44,800.

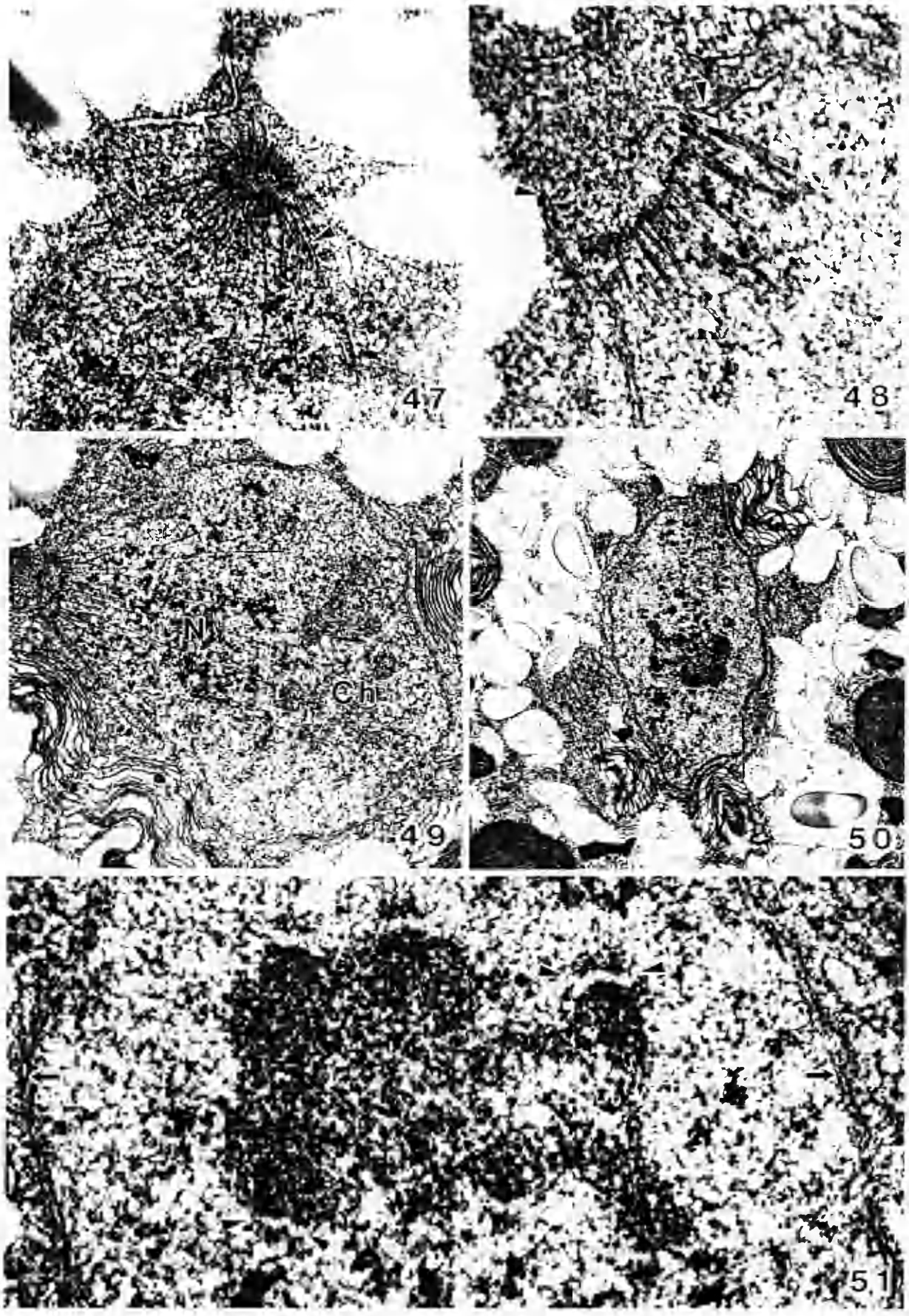
47
48
N
Ch
49
50
51

Fig. 52. Nucleolar material and chromatin intermix and migrate simultaneously to division poles. Note the kinetochore (arrowhead) within the traveling mass. x 21,000.

Fig. 53. Anaphase. Golgi bodies appear to be very active throughout mitosis. x 7,100.

Fig. 54. Late anaphase showing relatively shore interzonal midpiece (IZM) between traveling masses. x 12,200.

Fig. 55. MTOC begins to show a more spherical morphology during late anaphase. Microtubules are again seen to emanate away from the nucleus. x 38,000.

Fig. 56. Late anaphase-early telophase. Note the vacuole (V) pressed up against the nuclear envelope. x 16,800.

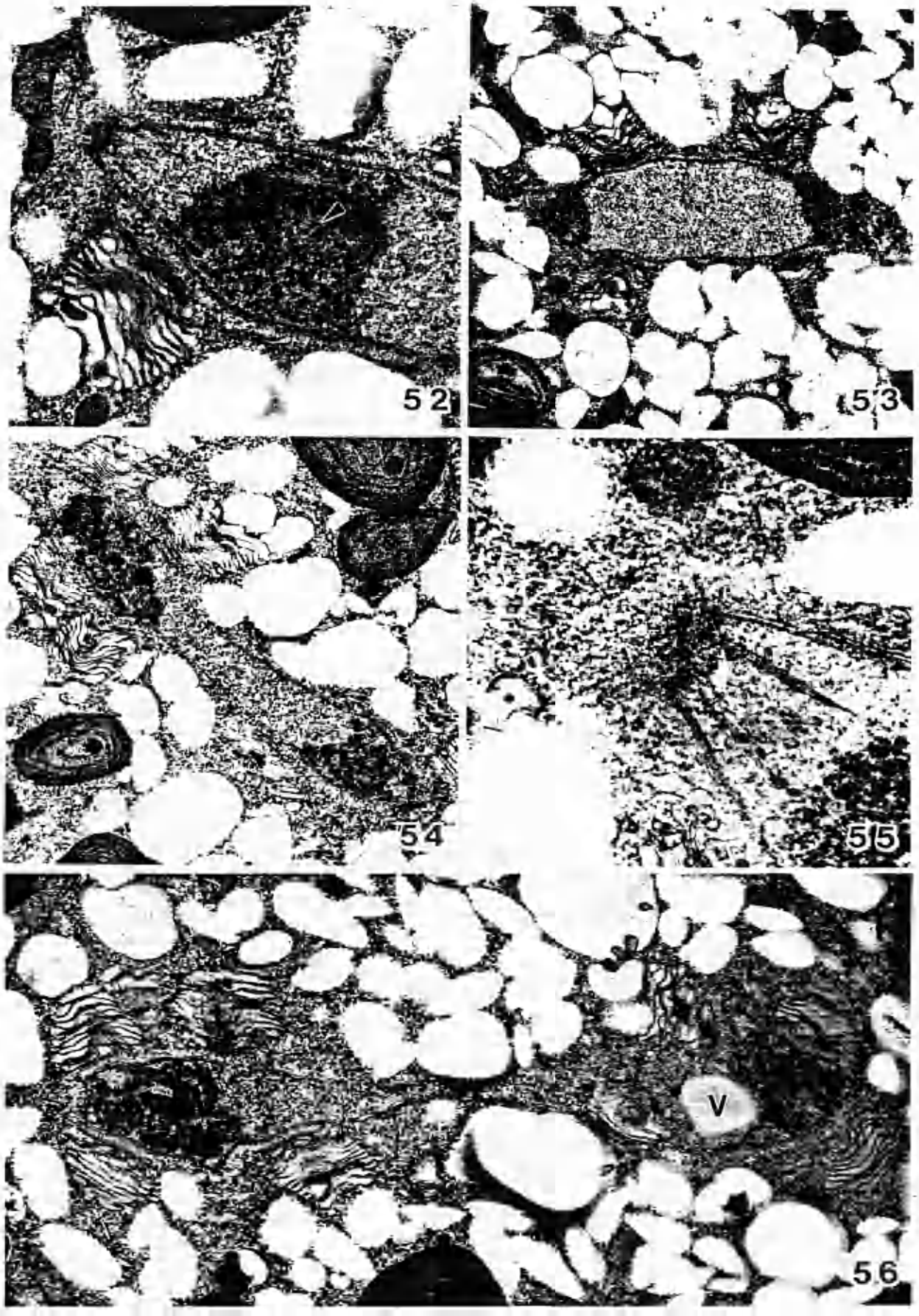
5 2
5 3
5 4
5 5
V
5 6

Fig. 57. Telophase. MTOC material (arrowheads), having become separate from nuclear envelope, again shows a spherical morphology. x 5,800.

Fig. 58. Telophase. A cleavage furrow (arrows) appears perpendicular to the poles of division as the nuclear envelope forms around the daughter nuclei. x 5,800.

Fig 59. Telophase. Nucleolar material reforms into an interphase-like condition as the cleavage furrow (arrows) further constricts. Note that the MTOC material (arrowhead) is still present next to the daughter nuclei. x 5,800.

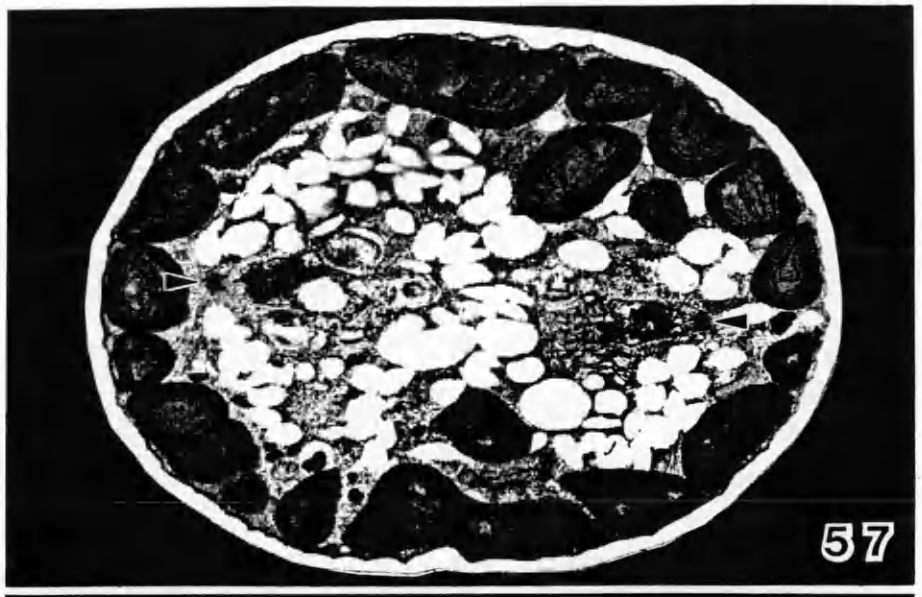
57

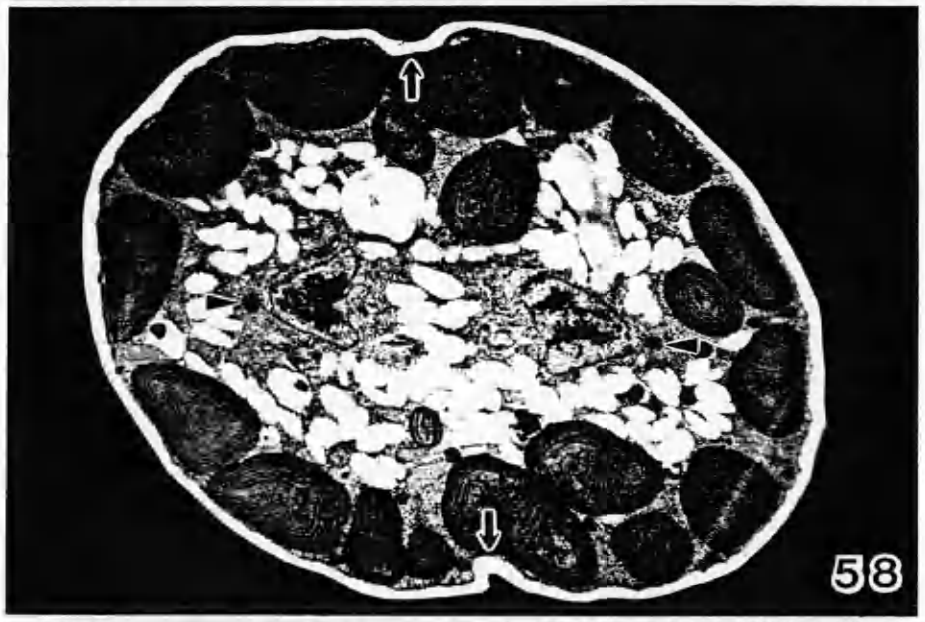
58

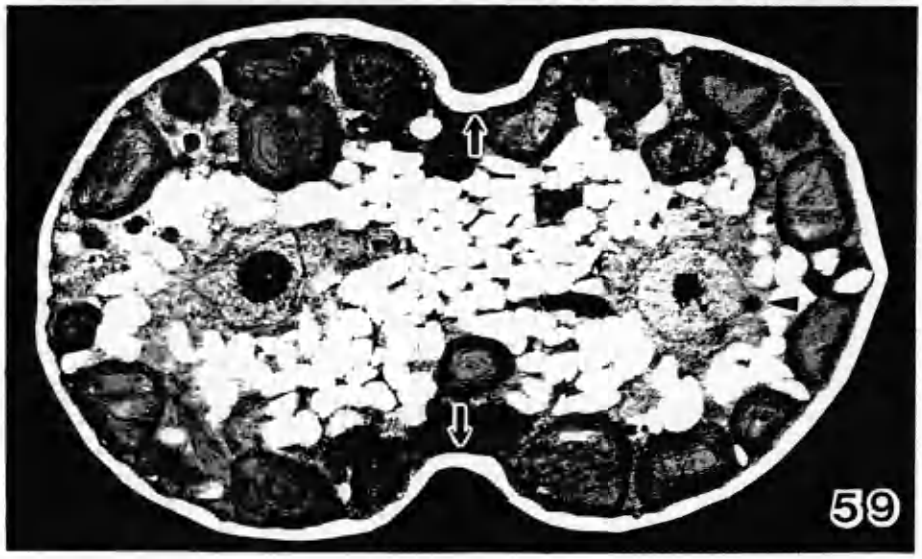
59

Fig. 60. Nomarski DIC with India Ink. Distribution of mucilaginous sheath between sides of cleavage furrow. x 600.

Fig. 61. Daughter nuclei (Nu) are situated in the approximate middle of the incipient daughter cells during late cytokinesis. Note the dumbbell morphology of dividing cell. x 7,800.

Fig. 62. A cytoplasmic bridge may be seen immediately after cytokinesis. x 600.

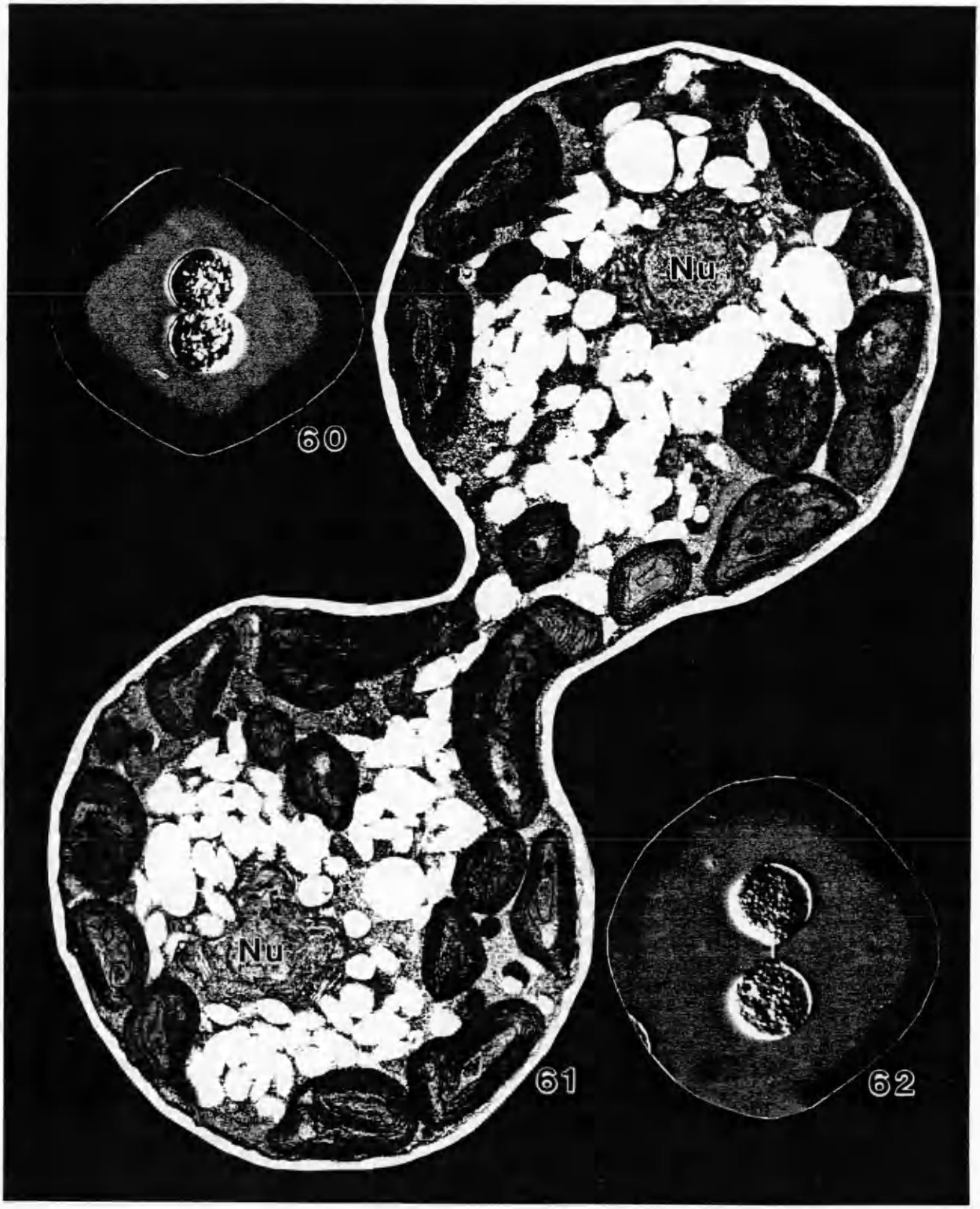
Nu
60
Nu
61
62

VITA

Born in Tuscaloosa, Alabama on December 28, 1968. After moving multiple times and attending many schools, settled in Hampton, Virginia and entered the College of William and Mary in 1987. After acquiring a BS in Biology in June of 1991, began MA program in the Department of Biology at the College of William and Mary. Studies were supported by a teaching assistantship in biology, 1991-1993. Awarded a fellowship and will matriculate into the Ph.D. program in Biophysics in August of 1993, at the Medical College of Wisconsin, Milwaukee, Wisconsin.